https://dx.doi.org/10.4314/dujopas.v9i4b.10
ISSN (Print): 2476-8316
ISSN (Online): 2635-3490
Dutse Journal of Pure and Applied Sciences (DUJOPAS), *Vol. 9 No. 4b December 2023*

Review of Recent Advances in Plant-Mediated Synthesis and Applications of $3d^6$- $3d^{10}$ Metal Oxide Nanoparticles and their Composites

Nnenna Winifred Odozi [1], Msenhemba Moses Mchihi [1, 2], Abimbola Modupe Olatunde[1]

[1]Department of Chemistry,
University of Ibadan,
Ibadan, Nigeria.

[2] Department of Chemical Science,
Yaba College of Technology
Lagos.

Email: mosesmsenhemba@gmail.com

Abstract

The aim of this review is to analytically discuss recent trends on the use of plant extract as environmental friendly technique for synthesis of $3d^6$- $3d^{10}$ metal oxide nanoparticles and composites employed for various applications. Nano-sized particles of some metal oxide and their composites have proven to be efficient for various applications in diverse fields such as wastewater treatment, luminescence, catalysis, solar cells, heat transfer systems, supercapacitors, medicine, sensors and corrosion inhibition. The nano forms of metal oxides such as oxides of Fe, Co, Ni, Cu and Zn are more valuable, excellent and proficient for various applications than their bulk counterparts owing to their specific chemical and physical characteristics. Synthetic techniques such as laser ablation, hydrothermal, sol-gel and physical grinding have been employed to synthesize these nanoparticles. Some of these techniques require much time, the use of toxic chemicals, instruments that are expensive and sophisticated skills. The use of plant extract for the synthesis of nanoparticles of transition metal oxides employed for various applications is effective, cheap, health friendly and simple. Even though agglomeration of nanoparticles synthesized via this approach is often reported, their efficacy for various applications overshadow this shortcoming which can be manipulated. Deductions from evaluation of some reports suggest that suitability of metal oxide nanoparticles for specific application depend on parameters such as crystal structure, crystalline size and morphology since metal oxide nanoparticles reported to be effective for specific application share similar attributes.

Keywords: Nanoparticles, synthesis, metal oxide, plant extract, application.

INTRODUCTION

Nanotechnology has received tremendous attention in the past two decades due to its diverse applications. Nanomaterials are widely used in corrosion inhibition, medicine, construction, sensors, catalysis and pollution control (Aslam *et al*., 2022; Fardood *et al*., 2017; Lu *et al*., 2019; Osuntokun *et al*., 2019; Chung *et al*., 2017). A nanomaterial is a material that has its size or at

**Author for Correspondence*

least one dimension in the nanoscale range of 1–100 nm (Baig *et al*., 2022). The characteristics of nanomaterials are considerably different compared to their bulk counterparts. More precisely, nanomaterials exhibit excellent quantum effects, mechanical properties, thermal and electrical conductivity compared to their bulk counterparts. A non-magnetic substance can become magnetic when reduced to the nanoscale range. In fact, even the color of certain elements in their bulk state is different from the color in the nanoscale range. A very good example is gold solution which appears yellowish as bulk material but appears red or purple when reduced to the nanoscale (Baig *et al*., 2022).

The prominence of materials with particle dimension within 1-100 nm in numerous applications is sequel to the tunability of their chemical, physical and biological properties resulting to enhanced efficacy over their bulk counterpart (Nwanya *et al*., 2021). High surface-to-volume ratio of nanoparticles makes them more reactive than the bulk materials since atoms on the surface tend to be more active than those at the center (Jayachandran *et al*., 2021). Reports on synthesis and application of different classes of nanomaterials such as metal based, carbon-based, nanocomposites and dendrimers are available in literature. Transition metal oxide nanoparticles have outstanding properties amid the metal oxide nanoparticles owing largely to their distinctive nature of outer d electrons. A nanoparticle is a particle which its dimensions are within the nanoscale range which is a scale that covers 1–100 nm (Baig *et al*., 2022). Metal oxide nanoparticles (especially those of Fe, Co, Ni, Cu and Zinc with 6, 7, 8, 9 and 10 electrons in their d orbitals respectively) are among the most used nanoparticles owing to special attributes such as enhanced band gap occasioned by alteration in surface characteristics, changes in structure that permit the variation of lattice symmetry, variation in electrochemical characteristics as a result of quantum confinement effect (Ahmad *et al*., 2022). Transition metals are elements that have partly filled d or f subshells in any of its common oxidation states. d block metals (comprising of 3d, 4d, 5d elements) and f block elements (which consist of lanthanoid and antinoids) makes up the transition metals. Some nanomaterials such as metal oxide nanoparticles are functionalized to obtain desired properties for specific applications. Functionalization of nanomaterials which may be covalent or non-covalent enhances dispersibility and efficacy for important applications. Some nanocomposites are produced via this approach. Nanocomposites are multicomponent materials with multiple different phase domains, in which at least one of the phases has at least one dimension in the order of nanometers.

Top-down and bottom-up techniques are employed to synthesize nanoparticles. Top down approach is achieved by reducing bulk material to nano size while bottom top technique deals with synthesis of nano materials from simpler units (Nwanya *et al*., 2021). Some of the conventional chemical and physical processes such as arc discharge method, sputtering, lithography, electrospinning, chemical vapor deposition, laser ablation and physical grinding that have been employed for the synthesis of transition metal oxide nanoparticles have many drawbacks occasioned by use of hazardous chemicals, expensive instrumentation, high energy requirement and complicated synthesis protocols that are bothersome to adopt for large scale production in the industry (Drummer *et al*., 2021). The need for simple and economically viable synthesis procedures that require the use of non-toxic chemicals have become imperative.

Plant extracts contain phytochemicals such as terpenoids, polyphenols, proteins, flavonoids, anthocyanidins, carotenoids, limonoids, glucosinolates, isoflavonoids, phytosterols that operate as reducing agents, hence play a vital role in the formation of nanoparticles. Therefore,

the composition of leaf extract has a considerable effect on green synthesis of nanomaterials. The use of extracts of different plant parts for synthesis of transition metal nanoparticles (which is the focal point of many researchers due to the very numerous applications) entails the use of extracts as reducing agent and transition metallic salt solution (Drummer *et al*., 2021). This approach is safe and economically viable, in that, the extracts of plants are non-toxic and the synthesis protocol shows tremendous prospects for large scale production. This approach is however, not devoid of drawbacks such as agglomeration of particles which is begging for attention. Reviews on the use of plant extracts for synthesis of transition metal nanoparticles have been reported. However, various conditions influencing green synthesis of metal nanoparticles as well as effect of compositing (or synergizing) for specific applications have not been fully explored. This paper focuses on review of works pertaining to the use of plant extract for synthesis of $3d^6$- $3d^{10}$ transition metal oxide nanoparticles (i.e oxides of Fe, Co, Ni, Cu and Zn), nanocomposites and their applications. Conditions that affect synthesis of nanoparticles of the aforementioned metal oxides as well as challenges and prospects are also discussed in this review.

Zinc oxide (ZnO) nanoparticles

ZnO is a semiconductor that is environmentally friendly. It has a broad band gap energy (3.3 eV) and n-type conductivity (Nguyen and Nguyen, 2020). The aforementioned attributes makes it suitable for different applications such as antibacterial agents, solar cells, corrosion inhibitors, photocatalysts, electronic devices and sensors (Nhu *et al*., 2022, Nguyen and Nguyen, 2020). Nano-sized ZnO has attracted tremendous attention of researchers in the recent years because it is quite easy to synthesize and has more interesting attributes compared to bulk ZnO.

Nanoparticles of ZnO have been synthesized using different plant extracts such as *Lippia adoensis* (Demissie *et al*., 2020), *Rosa indica* (Raj and Lawerence, 2018), *Cayratia pedata* (Jayachandran *et al*., 2021), *Myristica fragrans* (Faisal *et al*, 2021), *Eucalyptus globulus Labill* (Barzinjy & Azeez, 2020**),** *Salvia officinalis* **(**Abomuti *et al*., 2021), *Laurus nobilis* (Fakhari *et al*., 2019), *Albizia lebbeck* (Umar *et al*., 2019), *Ixora Coccinea* (Yedurkar *et al*., 2016), *Cassia fistula*, *Sambucus ebulus* (Alamdari *et al*., 2020), *Trifolium pratense* flower extract (Dobrucka and Długaszewska, 2016), *Nephelium lappaceum* peel extract (Karnan and Selvakumar, 2016), leaf extract of *Tamarindus indica* (Elumalai *et al*., 2015), *Parthenium hysterophorus* Leaf Extract (Datta *et al*., 2017), *Solanum nigrum* (Ramesh *et al*., 2015), aloe barbadensis miller (Sangeetha *et al*., 2011), extract of *saraca indica* leaves (Qu *et al*., 2011) and *Melia azadarach* (Naseer *et al*., 2020). Some plants that have been employed for synthesis of ZnO nanoparticles for various applications are presented in table 1. Generally, the synthesis of transition metal oxide nanoparticles involves mixing extracts of plants with transition metal precursor under specific conditions such as temperature, pH, reaction time, volume ratio of extract and metal precursor.

Jayachandran *et al* (2021) synthesized ZnO nanoparticles (in agglomerated form as revealed by Field Emission Scanning Electron Microscope) using aqueous leaf extract of *Cayratia pedata* and $Zn(NO_3)_2.6H_2O$. They estimated the average size of the synthesized ZnO nanoparticles to be 52.2 nm from results of X-ray diffraction studies using Scherrer's formula and the diffractogram showed crystal planes corresponding to lattice planes (100), (002), (101), (102), (110), (103), (112), and (201) in addition to hexagonal shape of the nanoparticles revealed from XRD analysis. The presence of Zn in the oxide form was also confirmed from Energy Dispersive Spectrum which revealed high signal for Zn and O with little traces of other

elements. Jayachandran *et al*., (2021) used their product for enzyme immobilization and the nanoparticles gave relative activity of 60% which is 88.2% of the activity in comparison with native ZnO immobilization. The phytochemicals in extracts of plants function as reducing agents for transforming the metal precursors to metal oxide nanoparticles. According to Jayachandran *et al*., (2021), the metal ions are encapsulated as an organic covering in some steps for their stabilization after reduction by plant extracts namely: 1. Activation phase (which involves metal ion reduction and nucleation of reduced metal ions) 2. Growth phase (which involves nanoparticles stability) and 3. The termination phase (where the shape of nanoparticles is established). This is summarized in figure 1. In some cases, the product is nanoparticles of metal (figure 5) instead of metal oxide nanoparticles, depending on the conditions employed for the synthesis.

Agglomerated zinc oxide nanoparticles

Agglomerated metal oxide nanoparticles are often said to be less efficient for various applications. Raj & Lawerence (2018) published their findings on green synthesis of agglomerated ZnO nanoparticles using aqueous extract of *Rosa indica* leaves and Zinc acetate dihydrate. They employed UV-Vis spectrophotometer, XRD analysis, Fourier Transform-Infra Red (FTIR),

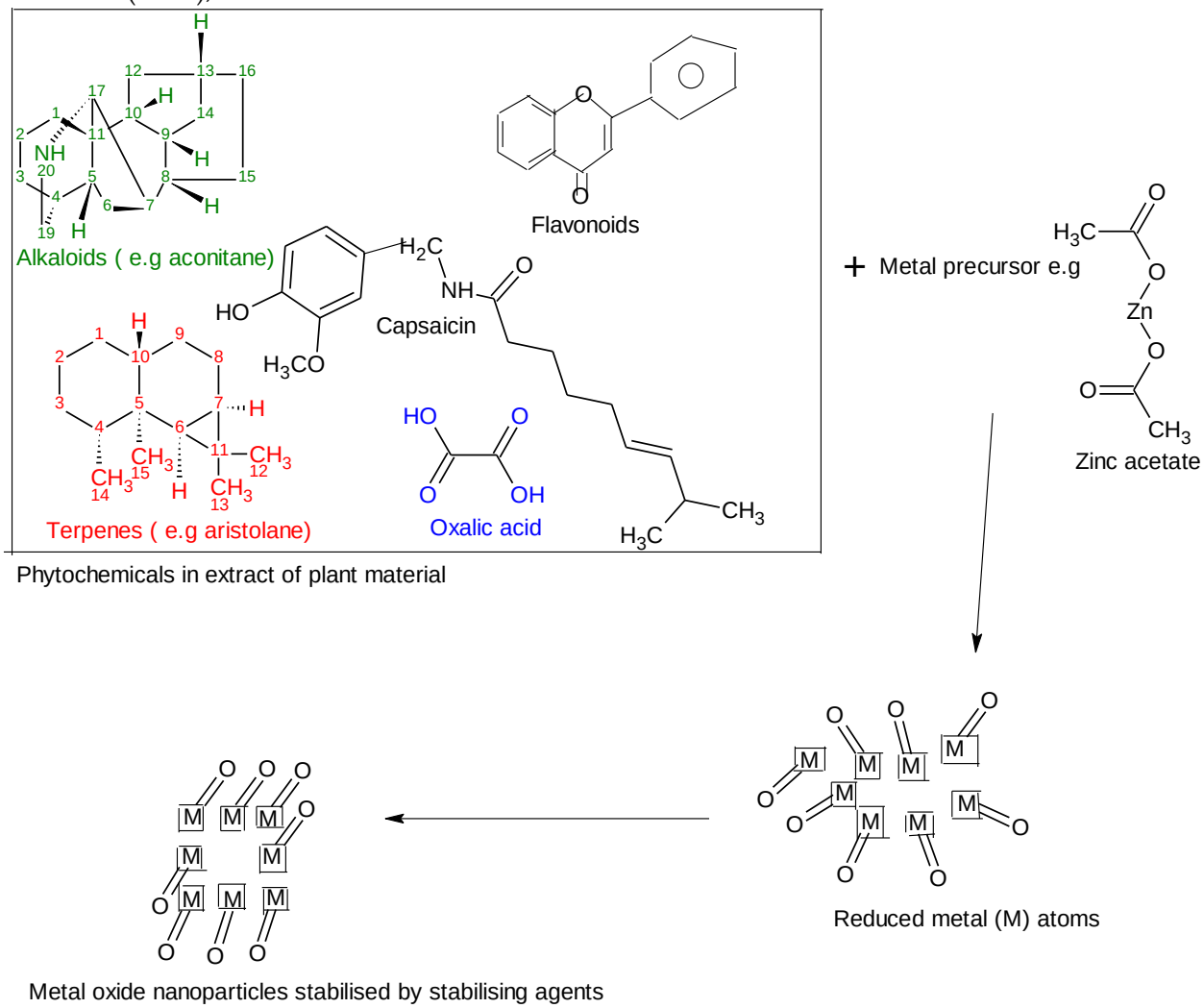

Figure 1. Mechanism for formation of metal oxide nanoparticles

Dynamic Light Scattering (DLS) and SEM with EDX for characterization of the green synthesized product. XRD peaks characteristic of ZnONPs were observed and the estimated crystallite size was found to be 35 nm using scherer's formula. FTIR spectrum showed a band at 572 cm^{-1} suggesting stretching vibration of ZnONPs. The agglomerated and spherical shaped ZnO nano-sized particles showed outstanding antibacterial activity against gram-negative and gram-positive bacteria. Studies conducted by Jayachandran *et al*., (2021) and Raj and Lawerence (2018) therefore suggest that green synthesized agglomerated nanoparticles are also efficient for some applications. Demissie *et al*., (2020) also reported green synthesis of agglomerated ZnONPs from *Lippia adoensis* leaf extract and zinc acetate dihydrate with excellent antibacterial active. The shape of the nanoparticles was found to be spherical from SEM results. They observed that the average crystallite size of the product decreased when the ratio of *Lippia adoensis* leaf extract increased and they asserted that the decrease in crystallite size with increase in extract volume was due to the fact that increase in extract volume gave rise to effective stabilization and capping which considerably decreased aggregation. Differential thermal analysis (DTA) and thermogravimetric analysis (TGA) revealed that the green synthesized ZnO nanoparticles which proved to be efficient antibacterial agent are thermally stable. Their work is in agreement with Jayachandran *et al*., (2021) and Raj and Lawerence (2018) which further buttressed the fact that agglomerated metal oxide nanoparticles are also suitable for various applications.

Effect of compositing on attributes of ZnONPs

Findings of several researchers suggests that compositing affects the shape of metal nanomaterials and efficiency of ZnO nanoparticles for a specific application. Gurgur *et al*., (2020) synthesized ZnO nanoparticles, ZnO–Ag and ZnO–Cu nanocomposites using eco-friendly dye extracted from *Bridelia ferrugine.* ZnO nanoparticles were flakelike in shape while ZnO–Ag and ZnO–Cu nanocomposites were spherical. The optical band gap for ZnO nanoparticles (3.24 eV) decreased to 3.18 on compositing with Ag and 3.13 eV for ZnO–Cu. This decrease in band gap for the Ag-ZnO nanocomposite compared to nanoparticles of ZnO is in agreement with the findings of Shreema *et al*., (2021) on synthesis of silver doped zinc oxide (Ag-ZnO) nanoparticles using leaf extract of Morinda citrifolia. This change in band gap would definitely alter suitability for applications like photocatalytic degradation. This is because semiconductors serve as catalysts for the comprehensive degradation of substances when excited by light with an energy value greater than their bandgap (Nhu *et al*., 2022). Among various semiconductors, TiO_2 and ZnO are widely employed as photocatalysts. In photocatalysis, catalyst and visible (or UV) light interact to produce reactive species like $OH^{\bullet}$ and $O_2^{\bullet-}$ that can interact with organic pollutants, triggering the removal of organic pollutants (Fagier, 2021). ZnO has a higher quantum efficiency compared to TiO_2 since it absorbs more energy in the ultraviolet region (Nhu *et al*., 2022). It is therefore unambiguous to mention that compositing alters properties of metal oxide nanoparticels.

Relationship between Metal precursor and application of synthesized ZnONPs

Critical survey of literature revealed that the metal precursor employed for synthesis of metal oxide nanoparticles does not affect the application of the synthesized metal oxide nanoparticles. Faisal *et al*., (2021) synthesized ZnO nanoparticles from aqueous fruit extracts of *Myristic fragrans* and $Zn(NO_3)_2 \cdot 2H_2O$. The average crystallite size estimated from XRD result was found to be 41.23 nm while SEM and TEM revealed spherical shaped particles. The product was found to be effective against α-glucosidase and α-amylase enzymes, larvae of A. aegypti, brine shrimps and was also found to be biocompatible with human red blood cells. The particles also degraded methylene blue dye. The degradation of methylene blue dye by

green synthesized ZnO nanoparticles reported by Faisal *et al*., (2021) is consistent with another study on degradation of methyl orange by ZnO nanoparticles synthesized using *Salvia officinalis* leaf extract and zinc nitrate solution (Faisal *et al*., 2021; Abomuti *et al*., 2021). Both XRD and Raman spectroscopy confirmed wurtzite hexagonal biosynthesized ZnO nanoparticles. The mean particle size of the biosynthesized nanoparticles was 26.14 nm ± 2.46 nm. The efficacy of the product as photocatalytic agent for degradation of methyl orange (MO) dye under UV light irradiation was evaluated and found to be excellent. They explained the process of photocatalytic degradation of methyl orange by ZnO nanoparticles based on the photogeneration of electron-hole pairs between the conduction and valence bands caused by UV light. Antifungal properties of the biosynthetic product were also probed. Excellent antifungal activity of the nanoparticles was reported and attributed to synergistic effect of the stabilised nanoparticles with flavonoids and tannins.

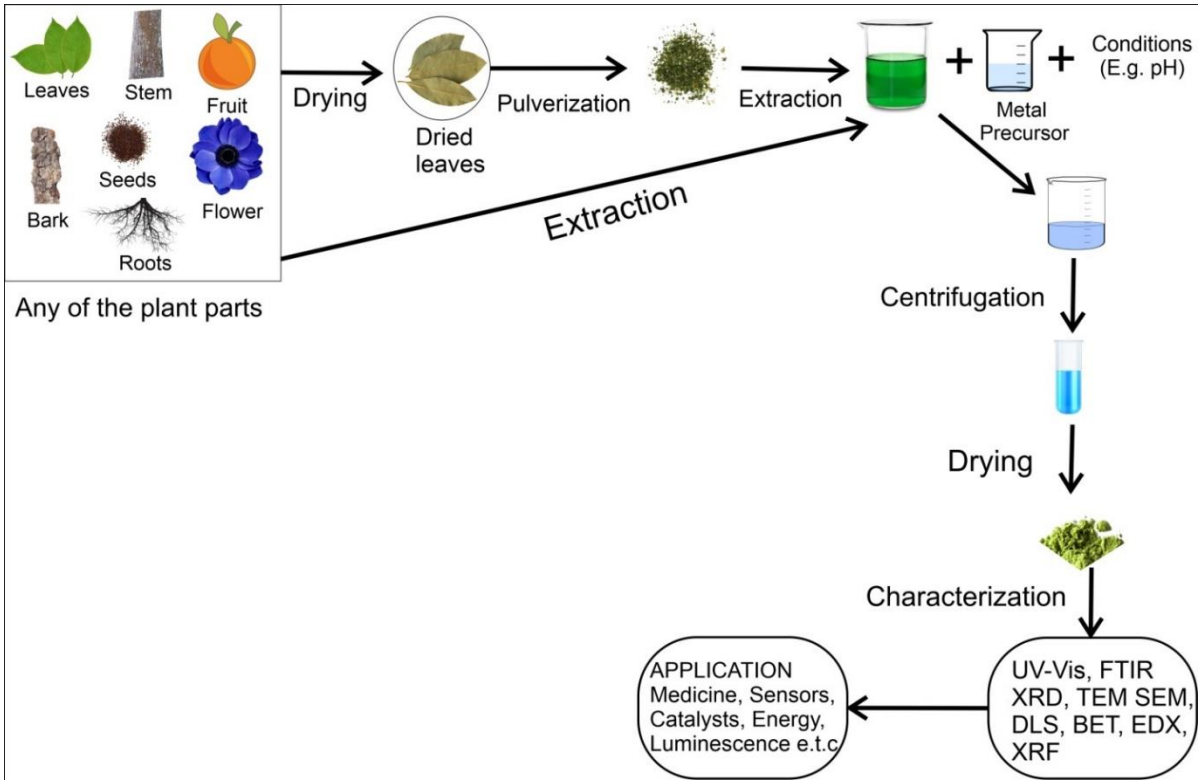

Figure 2. Plant-mediated synthesis, characterization and application of metal oxide nanoparticles.

General survey of current trends on synthesis and application of ZnONPs

Barzinjy & Azeez (2020) confirmed the synthesis of ZnO nanoparticles using leaf extract of *Eucalyptus globulus Labill* and zinc nitrate hexahydrate salt. 27 nm was the mean crystallite size of the nanoparticles computed from x-ray diffraction (XRD) analysis. Dynamic light scattering (DLS) studies revealed that the particle size of ZnO nanoparticles synthesized using environmentally friendly approach was found to be 32 nm. Differential scanning calorimetry (DSC) analysis showed that the green synthesized product requires more annealing to 365 °C so as to achieve very high purity and no significant weight loss was observed until 350 °C. They reported that most of the ZnO nanoparticles are hexagonal in shape with mean diameter of 35nm based on Scanning electron microscopic (SEM) analysis.

Fakhari *et al*., (2019) synthesized zinc oxide nanoparticles using zinc acetate and *Laurus nobilis L*. aqueous leaf extract. They went further to synthesize ZnO nanoparticles using a different precursor (which was zinc nitrate) and *Laurus nobilis L*. aqueous leaf extract. SEM images revealed spherical shaped nanoparticles for the two cases with different sizes (21.49 and 25.26 nm for ZnO nanoparticles synthesized using zinc acetate and zinc nitrate respectively). XRD results revealed that the mean crystallite size of ZnO nanoparticles derived from zinc acetate were smaller (25.26 nm) than ZnO nanoparticles synthesized from zinc nitrate (29.48 nm). They concluded that, the structure and surface morphology of ZnO nanoparticles are affected by precursors used.

Umar *et al*., (2019) employed $Zn(NO_3)_2{\cdot}6H_2O$ and stem bark aqueous extract of *Albizia lebbeck* for synthesis of ZnO nanoparticles $Zn(NO_3)_2{\cdot}6H_2O$. They employed spectroscopic and microscopic techniques for characterization. An absorption peak was observed at 370 nm in the UV-Vis spectrum. SEM micrographs revealed Spherical shaped agglomerated particles. 66.25, 82.52, and 112.87 nm was mean diameters for different concentrations (0.1 M, 0.05 M, and 0.01 M respectively). Results from DLS showed that the mean size of the particles synthesized using 0.05 M and 0.1 M zinc nitrate was 82.31 nm while that of 0.01 M was 110 nm. They probed the cytotoxic activities on human breast cancer cell lines in addition to antimicrobial and antioxidant activities. It was established that, the synthesized nanoparticles demonstrated tremendous cytotoxic effects and induction of membrane blebs on MCF-7 and MDA-MB 231 breast cancer cell lines which depended on concentration. The green synthesized nanoparticles of ZnO also showed excellent antioxidant activity in addition to antimicrobial activity against K. pneumoniae, S. aureus, B. cereus, E. coli and S. typhi. Synthesized nanoparticles of ZnO using leaf extracts of *Cassia fistula* and *Melia azadarach*. SEM micrographs for particles synthesized using both plants showed spherical shaped particles. Results of antibacterial activities revealed that nanoparticles synthesized using both plants show excellent ability against *Escherichia coli* and *Staphylococcus aureus* (Naseer *et al*., 2020).

Yedurkar *et al*., (2016) employed leaf extract of *Ixora coccinea* and zinc acetate for green synthesis of nanoparticles of ZnO. They used UV-vis, XRD, EDX, FTIR, DLS and SEM to confirm a successful synthesis. EDX confirmed the formation of highly pure nanoparticles of ZnO. The mean particle size of the green synthesized nanoparticles was found to be 145.1 nm from DLS analysis. −49.19 mV was the obtained value for zeta potential which suggested formation of stable ZnO nanoparticles since zeta potential above +30 mV or < −30 mV, imply stable suspensions. They concluded that, their product can be applied in medicals, catalysis, sensors, optical device, drug delivery, coatings, bio-technology and water remediation.

ZnO nanoparticles synthesized using leaves extract of *Pandanus Amaryllifolius* and zinc nitrate hexahydrate has been reported to be efficient inhibitor for corrosion of mild steel in acidic medium (Akhir *et al*., 2018). The nanoparticles with mean size of 16.25 nm demonstrated good corrosion inhibition behavior since corrosion inhibition efficiency of 79.43% was obtained from weight loss measurements (Akhir *et al*., 2018). Schematic representation of plant-mediated synthesis, characterization and application of metal oxide nanoparticles is presented in figure 2.

Table 1. Different conditions for green synthesis of ZnO nanoparticles

S/N	Plant name	Plant part	Extract Type	Metal salt	Calcination temperature (Ct) & time	Reaction time(Rt), Temperature (T) & pH	Mean crystallite size (MCS) & Particle size (PS)	Application	Reference
1	*Cayratia pedata*	Leaf	Aqueous	Zinc nitrate hexahydrate	Ct = 400 °C for 2h	Rt = 20 min, T = 65°C, pH = Not specified	MCS = 52.24 nm PS = not specified	Immobilization of enzyme	Jayachandran *et al*., 2021
2	*Rosa Indica*	Leaf	Aqueous	Zinc acetate dehydrate	Dried at 60 °C only	Rt= 20 min, T= 60°C, pH = 12	MCS = 35nm PS = 10nm	Antibacterial agent	Raj & Lawerence, 2018
3	*Lippia adoensis*	Leaf	Aqueous	Zinc acetate dehydrate	Ct = 400 °C for 1h	Rt= 2h, T= not specified, pH = 12	MCS = 26.7 nm, 22.6 nm, 18.5 nm for different volume ratio	Antibacterial agent	Demissie, *et al*., 2020
4	*Myristica fragrans*	Fruit	Aqueous	Zinc nitrate dihydrate	Ct = 500 °C for 2h	Rt = 2h, T= 60°C, pH = not specified	MCS = 41.23 nm. PS = 66nm	Antioxidant and photocatalytic agent	Faisal *et al*., 2021
5	*Eucalyptus globulus* Labill.	Leaf	Aqueous	Zinc nitrate hexahydrate	Ct = 400 °C for 2h	Rt = 2h, T= 60°C, pH = not specified	MCS = 27 nm PS = 32 nm	Adsorption of dyes, and heavy metal ions from aqueous systems	Barzinjy & Azeez, 2020
6	*Salvia officinalis*	Leaf	Aqueous	Zinc nitrate hexahydrate	Ct = 400 °C for 2h	Rt= 2h, T= 50°C, pH = 12	MCS = 11.89 nm, PS = 26.14 nm ± 2.46 nm	photocatalyt.ic and antifungal properties	Abomuti *et al*., 2021
7	*Laurus nobilis*	Leaf	Aqueous	Zinc acetate dehydrate & Zinc nitrate hexahydrate	Dried at 60 °C only	Rt = 2h, pH = 12	MCS = 29.48, & 25.26 nm PS = 21.49, 25.25 nm respectively	not specified	Fakhari *et al*., 2019
8	*Albizia lebbeck*	stem bark	Aqueous	Zinc nitrate hexahydrate	Ct = 350°C±10°C for 2h	Rt= 5h, T= 60°C, pH = 4, 6,8 & 10	MCS = 66.25, 82.52, & 112.87 nm for 1M, 0.05M, and 0.01M respectively	cytotoxic activities on human breast cancer cell lines, antimicrobial & antioxidant agents	Umar *et al*., 2019
9	*Ixora Coccinea*	Leaf	Aqueous	Zinc acetate dehydrate	Dried at 60 °C only	Rt= 2h, T= not specified pH = 12	MCS = not specified, PS = 145.1 nm	not specified	Yedurkar *et al*., 2016
10	*Cassia fistula* & *Melia azadarach*	Leaf	Aqueous	Zinc acetate dehydrate		Rt= 1h, T= 70°C, pH =	MCS = 2.72 nm for both. Ps = 68.1 nm & 3.62 nm respectively	Antibacterial agent	Naseer, *et al*., 2020).

Nanoparticles of Iron oxide

Iron oxide nanoparticles such as magnetite (Fe_3O_4) and maghemite (γ-Fe_2O_3) which is the oxidized form of Fe_3O_4 have been extensively applied in medicine (therapeutics drugs and medical diagnosis), photocatalysis, imaging techniques, sensors, superparamagnetic relaxometry etc. Different precursors of iron such as ferric chloride, iron nitrate, iron sulphate and extracts of different plant parts such as leafs, fruits, bark, stem, seeds, flowers, roots and husks have been employed to synthesize iron oxide nanoparticles (Buarki *et al*., 2022). High surface area, non-toxicity, superparagmagnetism and environmental compatibility are some of the interesting characteristics associated with Iron oxide nanoparticles synthesized using the green approach (Utsun, *et al*., 2022).

Polymorphism in Iron (III) oxide

Iron (III) oxide exhibits polymorphism, which is the phenomenon of existence of phases with the same chemical composition but different structure of crystals and therefore, physical properties (Tuček *et al*., 2015). α-Fe_2O_3, β-Fe_2O_3, γ-Fe_2O_3, ε-Fe_2O_3 and ζ-Fe_2O_3 phases are known. γ-Fe_2O_3 is ferrimagnetic and it is the second most stable polymorph of iron oxide while α-Fe_2O_3 is antiferromagnetic. α-Fe_2O_3 is the most thermodynamically stable polymorph of Fe_2O_3 under ambient conditions and it is majorly used in manufacture of steel, iron and other applications owing to its n-type semiconducting behavior (Bepari *et al*., 2014). High corrosion resistance nature of α-Fe_2O_3 has made it very useful for photo assisted electrolysis of water (Sahoo *et al*., 2010). Almost all phases of Fe_2O_3 undergo phase transformation when subjected to heat or pressure to form α-Fe_2O_3 which is the most thermodynamically stable. Polymorphs of Fe_2O_3 find applications in diverse areas owing to their distinct physical properties which is a consequence of crystal structure differences.

Recent trends in green synthesis and applications of iron oxide nanoparticles

Different Plants have been used to synthesize iron oxide nanoparticles for different applications. Hibiscus rosa sinensis (Buarki *et al*., 2022), leaf extract of *Ficus Carica* (Utsun, *et al*., 2022), root extract of *Mimosa pudica* (Niraimathee *et al*., 2020), extract of Iraqi grapes (Aziz *et al*., 2020), leaf extract of *Moringa oleifera* (Kiwumulo *et al*., 2022), leaf extract of *Bauhinia tomentosa* (Lakshminarayanan *et al*., 2021), and Hibiscus rosa-sinensis flowers (Razack *et al*., 2020) have been engaged to synthesize iron oxide nanoparticles. Table 2 shows some plants and conditions employed for synthesis of Fe, Cu, Co and Ni oxide nanoparticles for various applications.

Green synthesized iron oxide nanoparticles as antibacterial agents

Buarki *et al*., (2022) published their findings on the use of aqueous extract of *Hibiscus rosa sinensis* flowers and iron chloride tetrahydrate ($FeCl_2.4H_2O$) for synthesis of iron oxide nanoparticles. Results from UV-Vis, TEM, XRD, FTIR confirmed the successful synthesis of α-Fe_2O_3 ((hematite). XRD revealed that the structure of α-Fe_2O_3 nanoparticles is tetragonal and the mean crystallite size was found to be 36.4 nm. The mean size of the Fe_2O_3 nanoparticles was found to be 51 nm from results of TEM analysis. For all volume ratios, they observed surface Plasmon resonance (SPR) band around 700 nm. The position of the SPR band depends on the state of aggregation, surrounding medium dielectric, the particle shape and particle size (Buarki *et al*., 2022). They observed an absorption band at 624 cm^{-1} in the FTIR spectrum of aqueous extract of Hibiscus rosa sinensis flowers which shifted to 597 cm^{-1} in the FTIR spectrum of the synthetic product, suggesting Fe–O stretches in Fe_2O_3. Buarki *et al*., (2022) evaluated the antibacterial activity of their product and found that it is good antibacterial agent capable of replacing antibiotics that are currently used.

Synthesis of antibacterial potent β-Fe_2O_3 nanoparticles using aqueous extract of Iraqi grape and iron (III) chloride ($FeCl_3$) was also established by Aziz *et al*., (2020). They achieved this by mixing 16.2 g of $FeCl_3$ in 100 mL of distilled water and 200 mL of Iraqi grape aqueous extract for 30 minutes at 80 ^oC. The product was subjected to 200 ^oC heat treatment for 2h. Single crystallite of cubic β-Fe_2O_3 phase formation was confirmed from XRD studies and the crystallite size was found to be from 29 to 34 nm. A strong peak was observed at 526 cm^{-1} and assigned to vibrations of Fe-O. 49 to 50 nm was the size range of the particles based on SEM analysis. Agar well diffusion technique was employed by Aziz *et al*., (2020) to probe the antibacterial activity of their product using gram-negative Escherichia coli and gram-positive bacteria, Staphylococcus aureus. They rationalized their findings by stating that oxidative

stress occasioned by reaction of O species might be the mechanism of DNA and protein damage in bacteria by β-Fe_2O_3 nanoparticles resulting to antibacterial activity.

Nanoparticles of Fe_3O_4 were synthesized by Kiwumulo *et al*., (2022) using Ferric chloride and aqueous leaf extract of Moringa oleifera. They mixed 80 mL of 0.6 M Ferric chloride solution with 20 mL of the aqueous extract of *Moringa oleifera* and placed in a thermostated water bath at 80 ^oC for 4h. UV–Vis, FTIR, SEM, EDX and XRD were used to confirm formation of nanoparticles of Fe_3O_4. They recorded 10 peaks whose positions corresponded to planes of Fe_3O_4 crystals from XRD analysis. Morphological analysis was conducted using SEM and showed spherical shaped nanoparticles with size equal to 16 nm. They observed iron peaks in EDX spectrum in addition to peaks of other elements such as Na, Al, Cl and asserted that, nanoparticles such as their product can be used for treatment of cancer, bacterial and viral infections (Kiwumulo *et* al., 2022).

Green synthesized iron oxide nanoparticles as antioxidant

Antioxidant active iron oxide nanoparticles were synthesized by Utsun, *et al*., (2022) using Iron (III) chloride hexahydrate ($FeCl_3{\cdot}6H_2O$) and leaf extract of *Ficus Carica*. Results from their XRD analysis showed the presence of peaks that suggested the presence of both γ-Fe_2O_3 and α-Fe_2O_3 nanoparticle. EDX result showed that 46.79% of their product was iron and 36.47% oxygen while the remaining percentage was other elements. They probed the antioxidant activity of the product using two different approaches and recorded tremendous ability of the product to capture free radicals. SEM analysis revealed agglomerated nanoparticles which they rationalized by stating that the agglomeration may have occurred due to the presence of hydrogen bonding in the bioactive compounds present in the leaf extract coupled with the low capping ability of the extract used.

Green synthesized iron oxide with superparamagnetic performance

Niraimathee *et al*., (2016) reported their findings on the use of *Mimosa pudica* root aqueous extract and Ferrous Sulphate ($FeSO_4{\cdot}7H_2O$) for synthesis of iron oxide nanoparticles. They established successful synthesis by characterizing the product using different techniques. Roots of *Mimosa pudica* contain mimosin (which can hinder lung and liver cancerous cells proliferation), tannin, calcium oxalate crystals and ash (Niraimathee *et al*., 2016). A sharp peak observed at 294 nm (with band gap = 4.217 eV) in the UV-Visible spectrum was said to confirm the presence of Fe_3O_4 nanoparticles. The mean crystallite size of the particles was found to be 25.6 nm from XRD analysis. SEM analysis revealed spherical shaped particles that were well dispersed with mean size equal to 67 nm. Superparamagnetic performance of the particles was established from magnetization measurements.

Green synthesized iron oxide nanoparticles for immobilization

Lakshminarayanan *et al*., (2021) synthesized Fe_2O_3 nanoparticles using Ferric chloride and aqueous extract of *Bauhinia tomentosa* leaf and applied the product for Diolein synthesis. They achieved the synthesis by adding 0.01 M Ferric chloride to extract of *Bauhinia tomentosa* leaf dropwise in the volume ratio of 1:1. XRD, Raman spectroscopy, FTIR, UV-vis, FESEM, DSC & Zeta potential test were used to confirm successful synthesis of Fe_2O_3 nanoparticles. Results from FESEM showed that the mean size of the synthesized Fe_2O_3 nanoparticles was 70 nm while Brunauer–Emmett–Teller (BET) surface area was found to be 48.8 m^2/g. They observed a characteristic peak at 328 nm in the UV-Vis spectrum and a peak at 555.7 cm^{-1} in the FTIR spectrum which was assigned to Fe–O stretches of Fe_2O_3 which strongly suggested the formation of Fe_2O_3 nanoparticles, which was further validated from Zeta potential

measurements where a potential of −16 mV was obtained. The product was used for immobilization of lipase and it greatly boosted 1,3-diolein synthesis (Lakshminarayanan *et al*., 2021).

Green synthesized iron oxide nanoparticles for fortification

Fe_3O_4 nanoparticles synthesized using aqueous extract of Hibiscus rosa-sinensis flowers has been used for fortifying wheat biscuits (Razack *et al*., 2020). Buarki *et al*., (2022) also reported the synthesis of iron oxide nanoparticles using aqueous extract of Hibiscus rosa-sinensis flowers but their product was used as antibacterial agent. Razack *et al*., (2020) performed the synthesis by adding equal volume of extract to mixture of Ferric and Ferrous chloride prepared in (2:1 volume ratio) followed by centrifugation at 200 rpm for 1h and then 7000 rpm for 15 min. SEM result revealed cubic crystal (spinel shaped) with mean particle size of 65 nm. They used the Fe_3O_4 nanoparticles to fortify wheat biscuits and were able to establish that the synthesized nanoparticles of Fe_3O_4 can be employed as fortificants of food. Interestingly, they also observed that the level of bacterial contamination was less in biscuits fortified with nanoparticles of Fe_3O_4 since bacterial growth was observed at a later date in Fe_3O_4 nanoparticles fortified biscuits compared to biscuits without Fe_3O_4 nanoparticles suggesting longer storage competence (Razack *et al*., 2020).

Copper oxide nanoparticles

Scientists have reported synthesis of nanoparticles of CuO for various applications using extracts of different plants. Some of the plants employed for synthesis of CuO nanoparticles include extract of *saraca indica* leaves (Prasad *et al*., 2017), Olea europaea leaf extract (Sulaiman *et al*., 2017), *Bauhinia tomentosa* leaves extract (Sharmila *et al*., 2018) and euphorbia Chamaesyce leaf extract (Maham *et al*., 2017). Deductions from comparison of some of these reports suggest that application of these nanoparticles depend on certain parameters. Photocatalytic activity of CuO nanoparticles has been reported by several authors. CuO nanoparticles synthesized by Surendhiran *et al*., (2021) and Ijaz *et al*., (2017) for photocatalytic application (in separate studies) were crystalline and the average crystalline sizes were found to be 17.66 nm and 16.78 nm respectively. Crystal structure and morphological attributes of the nanoparticles synthesized by these two groups of researchers agree with each other, suggesting that photocatalytic activity of metal oxide nanoparticles is closely related to crystal structure and morphology. Ijaz *et al*., (2017) synthesized nanoparticles of CuO by mixing 1.205 g of Copper (II) nitrate trihydrate $Cu(NO_3)_2.3H_2O$ with 0.3 g *Abutilon indicum* extract in 20ml of double-distilled water followed by stirring at 2000 rpm with the aid of a magnetic stirrer after which the sample was placed in a muffle furnace at 400^oC for 2-3 minutes and then it was finally calcined in a muffle furnace at 400 ^oC for 2h. XRD revealed hexagonal wurtzite structure of CuO. Ijaz *et al*., (2017) established that their product is a potent antioxidant, photocatalytic dye degradation and antimicrobial agent while Surendhiran *et al* (2021) recorded good performance of their product as photocatalyst and mild steel corrosion inhibitor in 3.5% of NaCl medium.

Leaf extract of *Catharanthus Roseus* and copper sulphate ($CuSO_4.5H_2O$) were employed for synthesis of copper oxide nanoparticles (Begum *et al*., 2019). The nanoparticles of CuO were synthesized by mixing 200 ml of 0.1 M $CuSO_4.5H_2O$ with 50 ml of aqueous leaf extract of *Catharanthus Roseus* for 3 h followed by maintaining the mixture at 150 ^oC for 12 h in an oven after which the resulting sample was calcined at 400 ^oC for 2h. Begum *et al* (2019) used UV-Vis, FTIR and XRD to characterize their product. A match between the XRD pattern obtained and JCPDS no: 48-1548 revealed monoclinic crystal system of CuO nanoparticles and the

average crystallite size was found to be 35 nm. UV-Vis spectrum of the sample showed absorption band at 310 nm. The product demonstrated considerably antibacterial activity (Begum *et al*., 2019).

Devi *et al*., (2021) probed the anticancer activities of nanoparticles of copper oxide synthesized from Copper (II) chloride dihydrate ($CuCl_2.2H_2O$) and leaf extract of *coix lacryma jobi*. They refluxed a mixture comprising of 30 ml of extract and 70 ml of 10 mmol $CuCl_2.2H_2O$ at 100 ^oC for 1 h with continuous stirring to achieve synthesis of the nanoparticles of copper oxide. The researchers observed a peak near 282 nm which suggested the presence of nanoparticles of CuO while XRD measurements revealed CuO nanoparticles with monoclinic crystal structure and estimated mean crystallite size equal to 25.2 nm.

Altikatoglu *et al*., (2017) reported green synthesis of copper oxide nanoparticles using aqueous leaf extract *ocimum basilicum* and $CuSO_4.5H_2O$. They synthesized copper oxide nanoparticles by mixing 100 ml of 1 mM $CuSO_4.5H_2O$ with 10 ml of extract and stirring for 4 h at room temperature after which the solution was aged for 15 h followed by drying in an oven at 60 ^oC. SEM revealed spherical shaped nanoparticles with particle size = 70 nm. Their product showed good antibacterial activity (Altikatoglu *et al*., 2017). A similar study was conducted by Andualem *et al*., (2020) who synthesized antibacterial active nanoparticles of copper oxide. They added 10, 30, and 50 g of copper (II) nitrate trihydrate to three different volumetric flasks containing 100 ml of aqueous leaf extract of *Catha edulis* maintained at 80^oC followed by continuous stirring on a magnetic stirrer until the color changed from deep green to deep brown. They centrifuged for 30 min at 1000 rpm, dried the precipitate in an oven at 150^oC and calcined at 400° C for 2 h (Andualem *et al*., 2020). 31, 1.39, and 1.45 eV were the energy band gap for CuO nanoparticles synthesized using 1 : 10, 3 : 10, and 1 : 2 ratios respectively.

Sukumar *et al*., (2020) reported the use of aqueous seed extract of Caesalpinia bonducella, 25% ammonia solution and 0.01 M Cupric nitrate trihydrate [$Cu(NO_3)_2 \cdot 3H_2O$] for synthesis of nanoparticles of copper oxide. The synthesized nanoparticles were characterized using X-ray photoelectron spectroscopy, UV-Vis, FTIR, SEM and XRD and used as modifier for surface of graphite electrode. The modified electrode was characterized electrochemically by square-wave voltammetry, chronoamperometry and cyclic voltammetry methods and used for electrochemical detection of riboflavin (vitamin B_2) to ascertain its electrocatalytic properties. Their product demonstrated good performance for application in electrochemical sensing and antibiotics.

Nickel oxide nanoparticles

Nickel based nanoparticles have received tremendous consideration owing to their distinctive properties such as excellent conductivity, chemical stability, antifungal, antibacterial, antiviral and catalytic properties (Tas *et al*., 2021). NiO is a transition metal oxide that is a p-type semiconductor with a band gap ranging from 3.6-4.0 eV and has a cubic lattice structure (Lefojane *et al*., 2020). It also has good electron transfer ability and chemical stability (Habtemariam and Oumer, 2020). Researchers have reported synthesis of nickel oxide nanoparticles for various applications. Wardani *et al*., (2021) published their findings on the synthesis of nickel oxide (NiO) nanoparticles using aqueous leaf extract of *geratum conyzoides* and $Ni(NO_3)_2$. They achieved synthesis of nanoparticles of NiO by adding the extract into $Ni(NO_3)_2$ solution with constant stirring for 6 h at 80 °C after which the colloid was heated at 120 °C and then centrifuged to obtain a gel that was calcined for 2 h at 450 °C to obtain a grey black powder. An absorption band (that was absent in the precursor and extract) was

observed at 324 nm in the UV-Vis spectrum of synthesized NiO nanoparticles and TEM analysis revealed 8-15 nm as the size of the NiO nanoparticles. Five diffraction peaks were observed in the XRD spectrum at 2θ positions matching NiO nanoparticles and the mean crystallite size was 11.5 nm. Their product proved to be potent as catalyst for reduction of methylene blue.

Haider *et al*., (2020) synthesized nanoparticles of NiO by mixing aqueous roots extract of ginger and garlic with 0.1 nickel nitrate using different ratios at pH 12 and 90 °C for 2 h. They centrifuged the precipitates formed for 10 min at 10,000 rpm, washed with deionized water and dried overnight at 90 °C after which UV-Vis, FTIR, XRD and SEM were employed to characterize the synthesized nanoparticles of NiO. Intensity of diffraction peaks observed for optimum volume ratio suggested hexagonal and face-centered cubic NiO with mean crystallite size of 32.9 nm for ginger and that of garlic was 29.92 nm. SEM analysis revealed spherical shaped particles with size < 50 nm. Both nanoparticles of NiO synthesized using garlic and ginger roots extract demonstrated excellent catalytic degradation and antibacterial activity (Haider *et al*., 2020).

Cobalt oxide nanoparticles

Co_3O_4 and CoO are two variants of cobalt oxide that have stable properties and are both useful for solar cell, catalyst, sensors, lithium-ion battery and magnet materials owing to their excellent properties (Sardjono and Puspitasari, 2020). Co_3O_4 is p-type semiconductor (and is antiferromagnetic) with a direct optical band gap of 1.48-2.19 eV (Waris *et al*., 2021). Aqueous leaf extract of *Annona muricata* and cobalt nitrate have been used to synthesize cobalt oxide (Co_3O_4) nanoparticles (Rose and Sheeja, 2021). 25 ml of extract was added to 100 ml of Cobalt nitrate drop wise from a burette and the mixture was heated for 2 h at 80 °C followed by centrifuging at 10,000 rpm to obtain precipitates that were washed and dried at 200 ^{0}C for 3 h. The synthesized Co_3O_4 were also incorporated in starch using solution casting method and showed absorption band between 330-350 nm in the UV-Vis spectrum. 27 nm and 31 nm were the mean crystallize sizes of Co_3O_4 nanoparticles and Co_3O_4-starch composite. Both products showed excellent performance for methylene Blue dye photo degradation, hence, good photocatalytic activity.

Palm kernel oil which contains about 82% saturated fatty acid has been used to synthesize nanoparticles of cobalt oxide doped with iron (Yonti *et al*., 2021). In a study conducted by Yonti *et al*., (2021), an aqueous solution of $CoCl_2 \cdot 6H_2O$ and $Fe(NO_3)_3 \cdot 9H_2O$ was added to a vessel containing potassium carboxylate (5 mL), resulting to formation of precipitates which were washed with distilled water and dried. In their second route, carboxylate solution from the saponification reaction between 19.8 g of oil and 30 mL of 1.375 mol/L KOH solution was employed and nitric acid was used to neutralize all the excess OH^- before addition of the metallic solution. XRD, EDX, TEM and FTIR of their products calcined between 400 °C and 600 °C revealed formation of nanoparticles of cobalt iron oxide with sizes between 9 and 22 nm (Yonti *et al*., 2021). Hafeez *et al*., (2020) reported the use of *Populus ciliata* (safaida) aqueous leaves extract and cobalt nitrate hexahydrate as cobalt precursor for synthesis of nanoparticles of Cobalt oxide (Co_3O_4). They heated a mixture of 30 ml of cobalt nitrate hexahydrate and 20 ml of the extract for 3h at 80 °C, followed by cooling after which the cooled solution was centrifuged for 15 min at 15 000 rpm. The supernatant was carefully decanted and the residue was dried in an oven at 60 °C. FE-SEM analysis revealed uniform particles with size between 25–35 nm while FTIR showed the presence of hydroxyl group of phenolic compounds, Co-O, carbonyl group, amide group and C–O of alcohols or phenols since peaks were observed at

3458 cm^{-1}, 533 cm^{-1}, 1622 cm^{-1}, 1381 cm^{-1} and 1082 cm^{-1}respectively. The crystallite size computed from XRD analysis was in the range of 40–50 nm. The synthesized nanoparticles of cobalt oxide were potent against gram positive and gram negative bacteria and antibacterial activity increased with increase in concentration of nanoparticles of cobalt oxide (Hafeez *et al*., 2020).

Table 2. Different plant extracts and conditions employed for synthesis of oxides of Fe, Cu, Ni and Co nanoparticles.

S/N	Plant name	Plant part	Extract Type	Metal precursor	Calcination temperature (Ct) & time	Reaction time(Rt), Temperature (T) & pH	Mean crystallite size (MCS) & Particle size (PS)	Application	Reference
1	Hibiscus rosa sinensis	Flower	Aqueous	Iron chloride tetrahydrate	Not specified	Rt & T not specified pH = 7	MCS = 36.4 nm PS = 51 nm	Antibacterial agent	Buarki *et al.*, 2022
2	*Ficus Carica*	Leaf	Aqueous	Iron(III) chloride hexahydrate	Dried at 80°C for 1 day	Rt = 1hr T = 70°C pH = 11	MCS not specified PS = 43–57 nm	Antioxidant agent	Utsun, *et al.*, 2022
3	*Mimosa pudica*	root	Aqueous	Ferrous Sulphate ($FeSO_4$ $7H_2O$)	Not specified	Rt = 20 min T = 60°C pH = 9	MCS = 25.6 nm PS = 67 nm	Drug delivery (is the expectation)	Niraimathee *et al.*, 2016
4	*Iraqi grape*	Fruit	Aqueous	Iron (III) chloride ($FeCl_3$)	Ct = 200°C for 2h	Rt = 30 min T = 80°C pH not specified	MCS not specified PS = 49-50 nm	Antibacterial agent	Aziz *et al.*, 2020
5	*Moringa oleifera*	Leaf	Aqueous	Ferric chloride	Not specified	Rt = 4hr T = 80°C	MCS not specified PS = 16 nm	Drug delivery (is the expectation)	Kiwumulo *et al.*, 2022
6	*Bauhinia tomentosa*	Leaf	Aqueous	Ferric chloride	Dried at 90°C for 2h	Not specified	MCS not specified PS = 70 nm	synthesis of 1,3-diolein	Lakshminarayanan *et al.*, 2021
7	Hibiscus rosa sinensis	Flower	Aqueous	Ferric &Ferrous chloride in 2:1 ratio	Ct = 400°C for 3h	Rt = 1hr T = Room temp. pH not specified	MCS = 6.19 nm PS = 65 nm	Fortificants in wheat biscuits.	Razack *et al.*, 2020
8	*Musa Ornata*	Flower	Aqueous	Ferrous Sulphate	Not specified	Rt = 8h T = 70°C- 80°C pH = 4. 5, 6, 7, 8, 9, & 10	MCS = 43.69 nm PS = 86.2 nm	Antibacterial agent	Saranya *et al.*, 2017
9	*Abutilon indicum*	Leaf	Aqueous	Copper (II) nitrate trihydrate	Ct = 400°C for 2h	Not specified	MCS = 16.78 nm PS = Not specified	antioxidant, photocatalytic& antimicrobial	Ijaz *et al.*, 2017
10	*Catharanthus Roseus*	Leaf	Aqueous	copper sulphate ($CuSO_4.5H_2O$)	Ct = 400°C for 2h	Rt = 12 h T = 150°C pH not specified	MCS = 35 nm PS = Not specified	Antibacterial agent	Begum *et al.*, 2019
11	*Coix lacryma jobi*	Leaf	Aqueous	Copper (II) chloride dihydrate	Ct = 300 °C for 1 h	Rt = 1 h T = 100°C pH not specified	MCS = 25.2 nm PS = Not specified	Anticancer agents	Devi *et al.*, 2021
12	*Catha edulis*	Leaf	Aqueous	copper (II) nitrate trihydrate	Ct = 400°C for 2h	Rt not specified T = 80°C pH not specified	MCS = 28.10, 25.30 & 18.20 nm for 3 ratios	Antibacterial agent	Andualem *et al.*, 2020
13	Aerva javanica	Leaf	Aqueous	copper chloride dehydrate	Dried at 60 ° C for 2 h	Rt = 2 h T = 80°C pH not specified	MCS = 15 nm PS = 50.1 nm	Antimicrobial & cytotoxic active	Amin *et al.*, 2021
14	*Caesalpinia bonducella*	Seed	Aqueous	Cupric nitrate trihydrate	Ct = 450°C for 1h	Rt = 7 h, T & pH not specified	MCS = 13.07 nm	Electrochemical applications	Sukumar *et al.*, 2020
15	*Annona muricata*	Leaf	Aqueous	cobalt nitrate	200 °C for 3 h	Rt = 2 h, T= 80 °C	MCS = 27 nm & 31 nm	Photocatalytic agent	Rose and Sheeja, 2021
16	*Populus ciliate*	Leaf	Aqueous	cobalt nitrate hexahydrate	60 °C	Rt = 2 h, T= 80 °C,	not specified	Antibacterial agent	Hafeez *et al.* 2020
17	*geratum conyzoides*	Leaf	Aqueous	Nickel nitrate $Ni(NO_3)_2$	Ct = 450°C for 1h	Rt = 6 h, T= 80 °C	MCS = 11.5	Catalyst	Wardani *et al.*, 2019

Conditions employed for green synthesis of nanoparticles of Fe, Cu, Ni and Co for various applications

Desired characteristics of nanoparticles such as shape, particle size, stability etc are principally attained by controlling the route of the synthesis (Saranya *et al*., 2017). It is imperative to regulate numerous factors such as pH, reaction temperature, reaction time, metal precursor concentration etc to synthesize nanoparticles with desired properties such as size and shape (Yusoff *et al*., 2019). Conditions that influence synthesis of nanoparticles of transition metal oxides are presented in figure 3.

pH

Researchers have established that pH of medium has a tremendous influence on properties of synthesized nanoparticles. Saranya *et al*., (2017) synthesized nanoparticles of iron oxide at pH equal to 4. 5, 6, 7, 8, 9, & 10. Maintaining the same precursor concentration and volume ratio, they observed peak of maximum absorbance for nanoparticles of iron oxide synthesized at pH = 9. Alkaline pH has been found to be generally suitable for synthesis of transition metal nanoparticles.

Zayyoun *et al*., (2016) synthesized nanoparticles of stable Cu_2O and CuO from the same precursor (which is copper acetate monohydrate) by varying pH of the reaction mixture using sodium hydroxide solution. At pH = 6.1, an orange color was observed which confirmed the formation of Cu_2O nanoparticles and when this sample was analyzed using XRD, peaks at 2θ position corresponding to the crystalline phase of Cu_2O were observed. When the pH was raised to basic region, a blue coloration was observed suggesting variation in Cu^{2+} chemical environment and the solution color finally changed to black when the pH was 12, indicating the formation of CuO nanoparticles. TEM analysis of CuO revealed spherical shaped nanoparticles with 4.5 nm average diameter while nanoparticles of Cu_2O were cubic with average diameter = 3 nm.

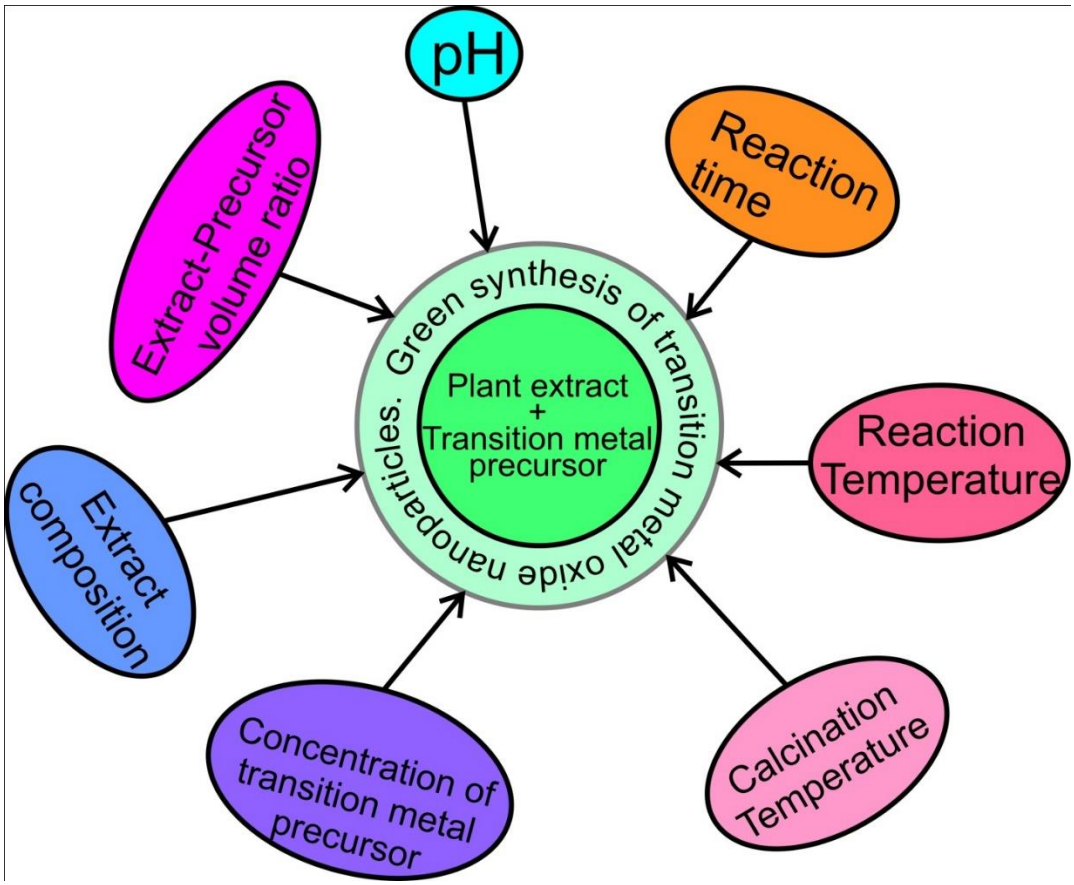

Figure 3. Conditions that affect synthesis of transition metal oxide nanoparticles.

In their published work on Synthesis of Biocompatible Fe_3O_4 Nanoparticles at pH 11.33, 12.15, 11.94 and 12.25, Yusoff *et al*., (2019) established that solution pH plays an important role on crystallite size. From pH 11.33 to 12.15, they observed that, the crystallite size decreased with increase of pH but increased spectacularly above 12.15. Bashir *et al*., (2013) synthesized

nanoparticles of iron oxide at different pH (1 and 4). They observed peaks corresponding to Magnetite and hematite phases. The magnetite phase transformed to maghemite when the pH was increased; an observation that was rationalized by asserting that increase of concentration of hydroxyl ion caused reduction in Fe^{2+} ions and increase in Fe^{3+} ions.

pH also affects application of synthesized transition metal oxide nanoparticles in diverse areas. The effect of pH on the removal of copper from wastewater using green synthesized nanoparticles of ZnO has been reported (Primo *et al*., 2020). Primo *et al*., (2020) asserted that, the number of active sites on the surface of ZnO (adsorbent) increases with corresponding increase in pH of the solution, ensuing in higher efficiency of adsorption. They probed the stability of ZnO at two different pH values (4 and 6) after removal of Cu and discovered that there was a little increase in weight which differed with pH compared to the original weight. They also established that the crystallite size after adsorption increased with increase in pH after estimating the crystallite sizes of two different samples after adsorption at pH 4 and 6. Akhtar *et al*., (2021) reported that bacteria produce organic acids (such as amino acids, sulphuric acid, nitric acid, ascorbic acid) by altering the pH of the culture broth and solubilizing the zinc ions.

Temperature

Effect of temperature on green synthesis of nanoparticles of ZnO has been reported (Basri et al., 2020). Maintaining the pH of the solution at 12, Basri *et al*., (2020) synthesized nanoparticles of ZnO at 28^{o}C and 60^{o}C using aqueous extract of dried pineapple peels and $Zn(NO_3)_2 \cdot 6H_2O$. FESEM analysis of particles synthesized at 28^{o}C revealed a mixture of rod-shaped and spherical particles with diameter in the range of 8-46 nm and less agglomeration while mixture of agglomerated rod-shaped and spherical nanoparticles were observed for particles synthesized at 60^{o}C with diameter in the range 73-123 nm. They stated that increase in temperature can increase frequency of collision and increase agglomeration of the nanoparticles of ZnO. Jayachandran *et al*., (2021) attempted to synthesize nanoparticles of ZnO using extract of plant and zinc nitrate at 55 ^{o}C, 65 ^{o}C and 75 ^{o}C. They reported that, successful synthesis was achieved at 65 ^{o}C as there was no reaction at 55 ^{o}C while ashes were formed at 75 ^{o}C.

Aziz & Bronny (2019) pubished their findings on synthesis of ZnO nanoparticles at 50 ^{o}C, 60 ^{o}C, 70 ^{o}C, 80 ^{o}C and 90 ^{o}C at the same pH = 12. They observed an increase in the crystalline size with corresponding increase in temperature (i.e 15.06 nm, 15.98 nm and 16.50 nm for nanoparticles synthesized at 50°C, 60°C and 70°C respectively). A decrease in crystallite size was however observed at 80 ^{o}C (i.e 14.46 nm) but the crystallite size further increased to 26.03 nm when the temperature was raised.

Extract composition

Different plants contains different amount of bioactive compounds that act as reducing and stabilization agents for the synthesis of nanoparticles of transition metal oxide. It is therefore expected that the reducing ability of extracts of different species of plant will differ (Xu *et al*., 2021). Some of the compounds present in extracts of plant parts are presented in figure 4. Naseer, *et al*., (2020) compared synthesis of nanoparticles of ZnO using the same precursor and leaf extracts of *Cassia fistula* and *Melia azadarach*. They discovered that, the average diameters of ZnO nanoparticles synthesized using *Cassia fistula* was 68.1 nm while the average diameters of ZnO nanoparticles synthesized using *Melia azadarach* was found to be 3.62 nm, which suggested that *Melia azadarach* was more efficient for synthesis of small nanoparticles

of ZnO compared to *Cassia fistul.* The efficiency was attributed to the fact that *Melia azadarach* contains more phytochemicals compared to *Cassia fistula.* Synthesis of nanoparticles of iron using Mangifera indica, Azadiracta indica Murraya Koenigii, and Magnolia champaca with the same iron precursor ($FeSO_4$) has been reported (Devatha *et al*., 2016). In the study, SEM analysis revealed that the nanoparticles synthesized using the four different plant extracts have different sizes and their phosphate removal efficiency also varied, suggesting that composition of extract influences the synthesis of nanoparticles and hence, properties (Devatha *et al*., 2016).

Extract-metal precursor volume ratio

Buarki *et al*., (2022) synthesized iron oxide nanoparticles using 1:1, 1:2 and 1:3 volume ratios of $FeCl_2.4H_2O$ to extract of *Hibiscus rosa sinensis* flowers respectively. For all the volume ratios,

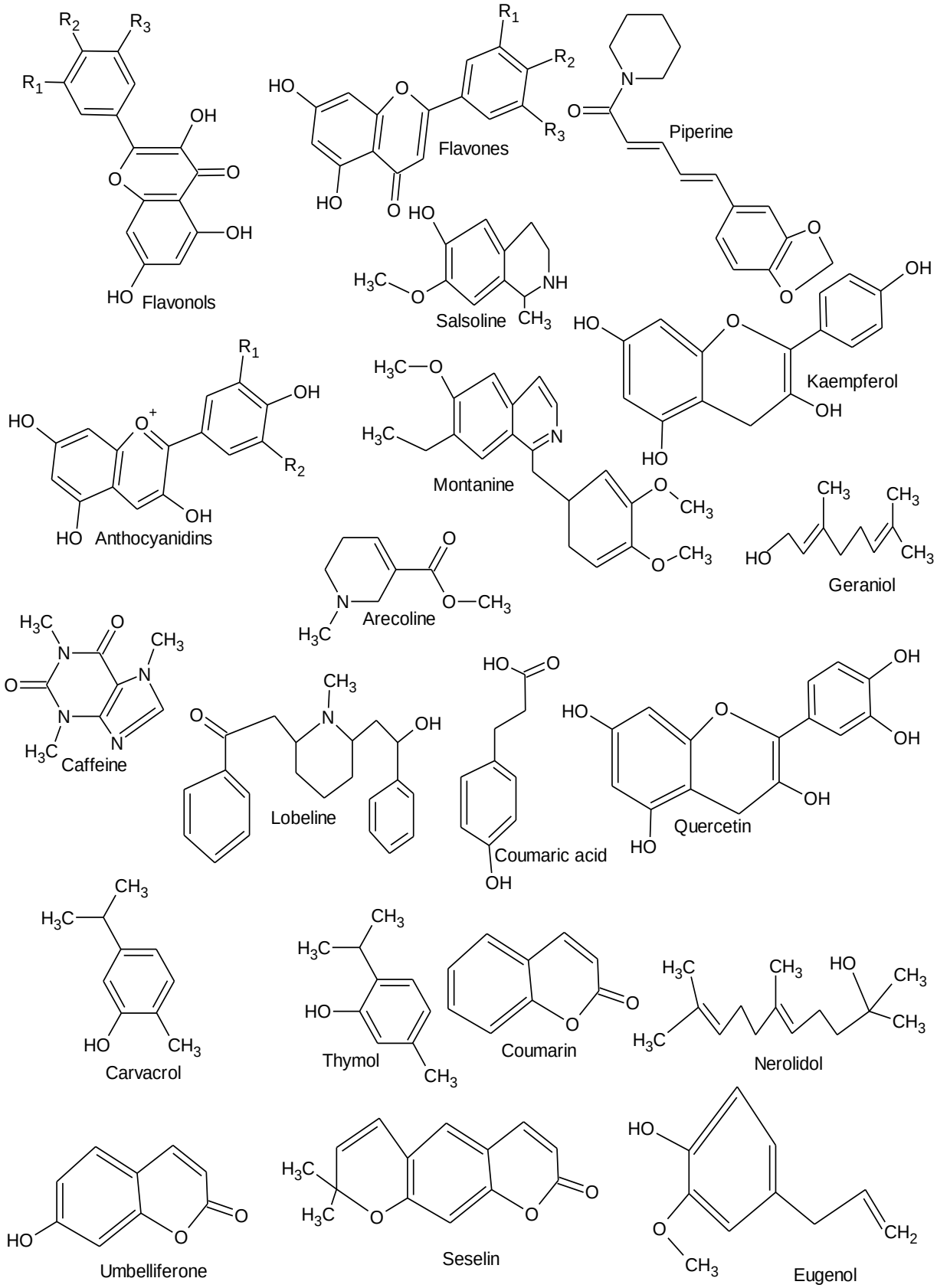

Figure 4. Some compounds in extracts of plants

UV-Vis analysis showed SPR around 700 nm but the highest absorption peak was observed for nanoparticles synthesized using 1:2 volume ratio. They also discovered that activity of the nanoparticles also differ with volume ratio and claimed the differing antibacterial activities may be related to difference in the number of particles in solution and the size as smaller particles have larger surface area (Buarki *et al*., 2022).

1:1, 3:2 and 9:1 extract-metal precursor volume ratios were used for synthesis of ZnO nanoparticles in a study (Demissie, *et al*, 2020). The researchers reported that different mean crystallite sizes were obtained from XRD measurements for all the different volume ratios used and the value for Band-gap energy for 9 : 1, 3 : 2, and 1 : 1 volume ratios were 3.05, 3.11, and 3.21 eV respectively.

Concentration and nature of metal precursor

Concentration of metal precursor greatly affects synthesis of nanoparticles of transition metal oxide. In their research on the use of *Citrus Medica Linn* Extract for bio-sythensis of nanoparticles of copper, Pradhan *et al*., (2020) observed a more intense absorption peak in UV-visible spectrum of nanoparticles synthesized using 1mM $CuSO_4$ compared to nanoparticles synthesized using 5 mM and 9 mM $CuSO_4$ which (according to them) was due to smaller sized nanoparticles formation. 1mM was therefore considered as the optimum concentration for synthesis. They also observed a bathochromic shift and broadening with increase in concentration of the metal precursor which they rationalized by asserting that, more Cu ions participated in the reduction reaction resulting to nanoparticles agglomeration. Guzman *et al*., (2021) also reported their findings on concentration effect on the synthesis of nanoparticles of copper oxide and concluded that, particle size, morphology and crystalline properties of nanoparticles vary with changes in conditions including concentration. Their product exhibited some properties (like good antibacterial activity, crystalinity) similar to copper oxide nanoparticles synthesized by Amin *et al*., (2021).

Tremendous efforts have been recorded in respect of conditions (such as pH, reaction temperature, reaction time, metal precursor concentration and extract composition) that influence the synthesis of metal oxide nanoparticles. However, the relationship between metal oxide nanoparticles at specific conditions and suitability for specific applications is yet to be explored fully.

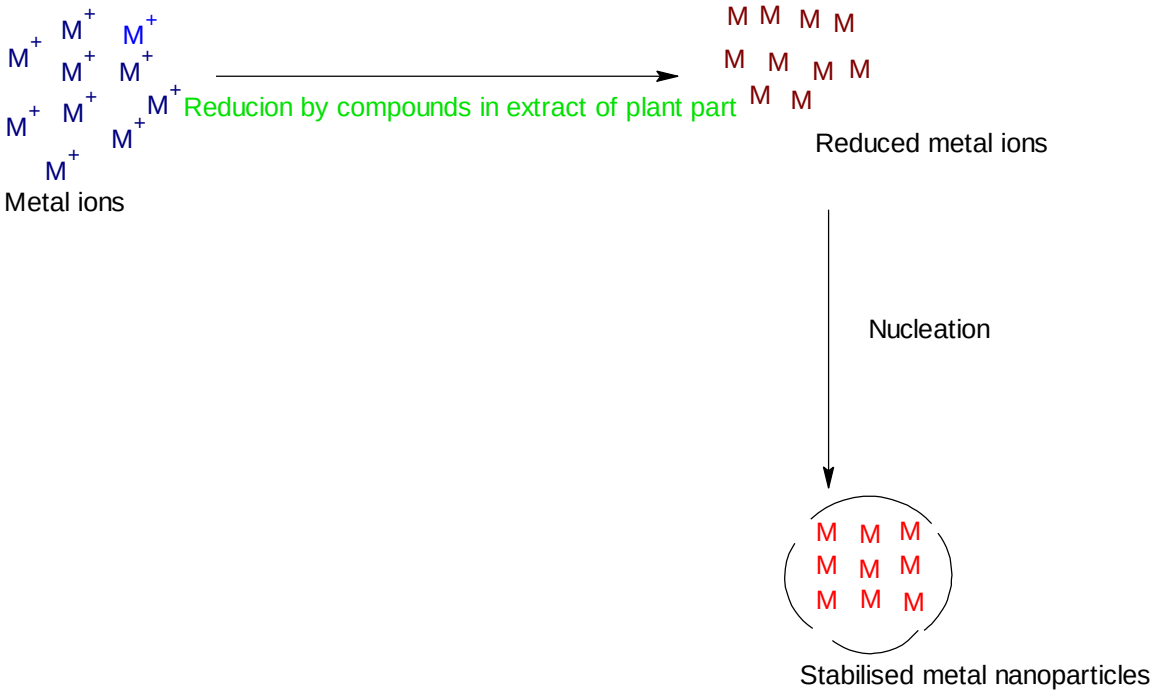

Figure 5. Mechanism for formation of metal nanoparticles

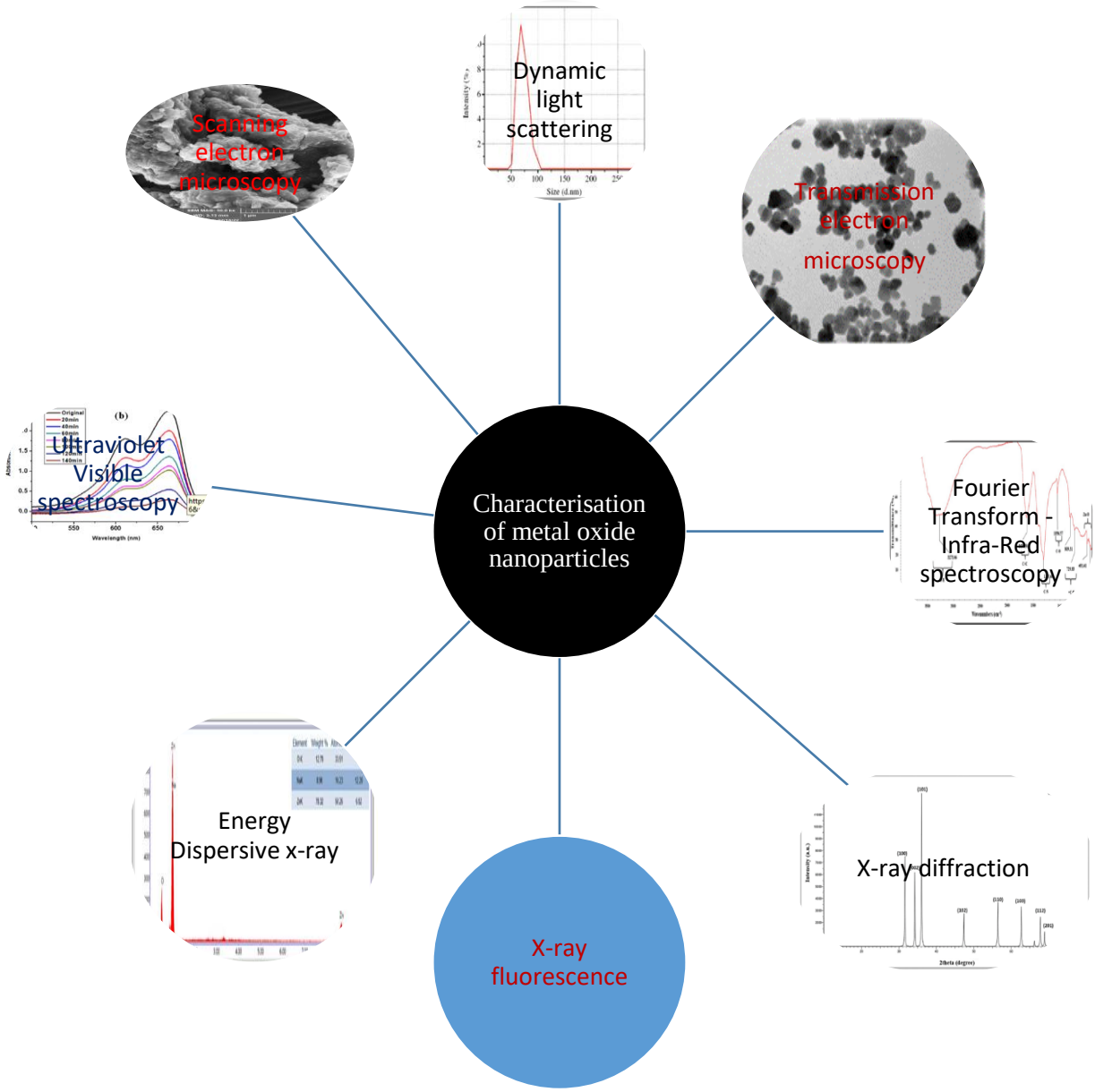

Figure 6. Techniques for characterization of metal oxide nanoparticles synthesized via plant-mediated approach

Challenges and Prospects

Achieving controlled synthesis for high quality nanoparticles that are structurally pure via the use of plant extract approach is currently a challenging task that needs unprecedented attention. Aggregation of nanoparticles is also one of the major drawbacks associated with the use of extract of plant materials for synthesis of metal oxide nanoparticles. Researchers should therefore, seek techniques that would overcome this challenge. This is important because

aggregated nanoparticles are suitable for certain applications but less effective for other applications.

Several researchers have employed sophisticated techniques such as UV visible spectrometer, Scanning electron microscopy, Transmission electron microscopy, X-ray diffraction, Dynamic light scattering and x-ray fluorescence among others as presented in figure 6 for successful characterization of metal oxide nanoparticles synthesized via plant-mediated approach. However, Critical review of literature revealed that researchers have paid less attention to full screening of extracts of plants used for synthesis of metal oxide nanoparticles. Consequently, less is said of the actual compounds that are likely to be responsible for stabilizing nanoparticles of metal oxides. Sophisticated techniques like High-performance liquid chromatography (HPLC) should be employed in addition to FTIR, UV-Visible spectroscopy and other techniques to comprehensively identify compounds in the extract that are responsible for stabilization and formation of nanoparticles of metal oxides. In addition, much has not been reported on commercialization of metal oxide nanoparticles synthesized using plant-mediated approach.

Regardless of the shortcomings (figure 8) associated with plant-mediated synthesis of nanoparticles of metal oxide, this synthetic approach seem to be promising for industrial scale synthesis of metal oxide nanoparticles for various applications since the method is environmental friendly, inexpensive and simple. Much progress have been recorded and outstanding breakthroughs are likely to be recorded in the near future in diverse areas including (but not limited to) aeronautics, textiles, computer, construction, petroleum, cosmetics, pollution control, medicine, robotics, agriculture, education and automobile industries as represented in figure 7.

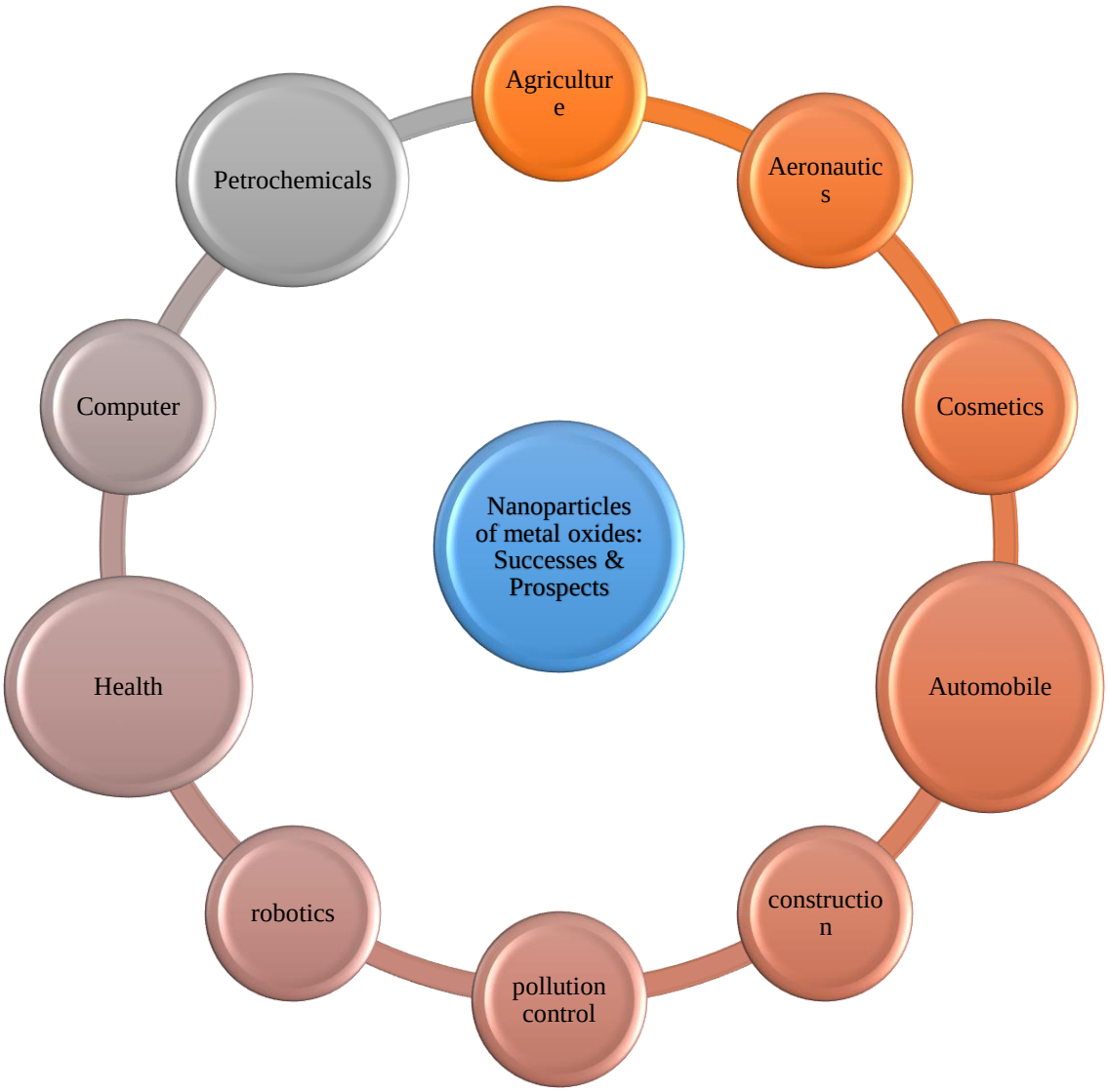

Figure 7. Successes and prospects of metal oxide nanoparticles synthesized using plant-mediated approach in diverse industries

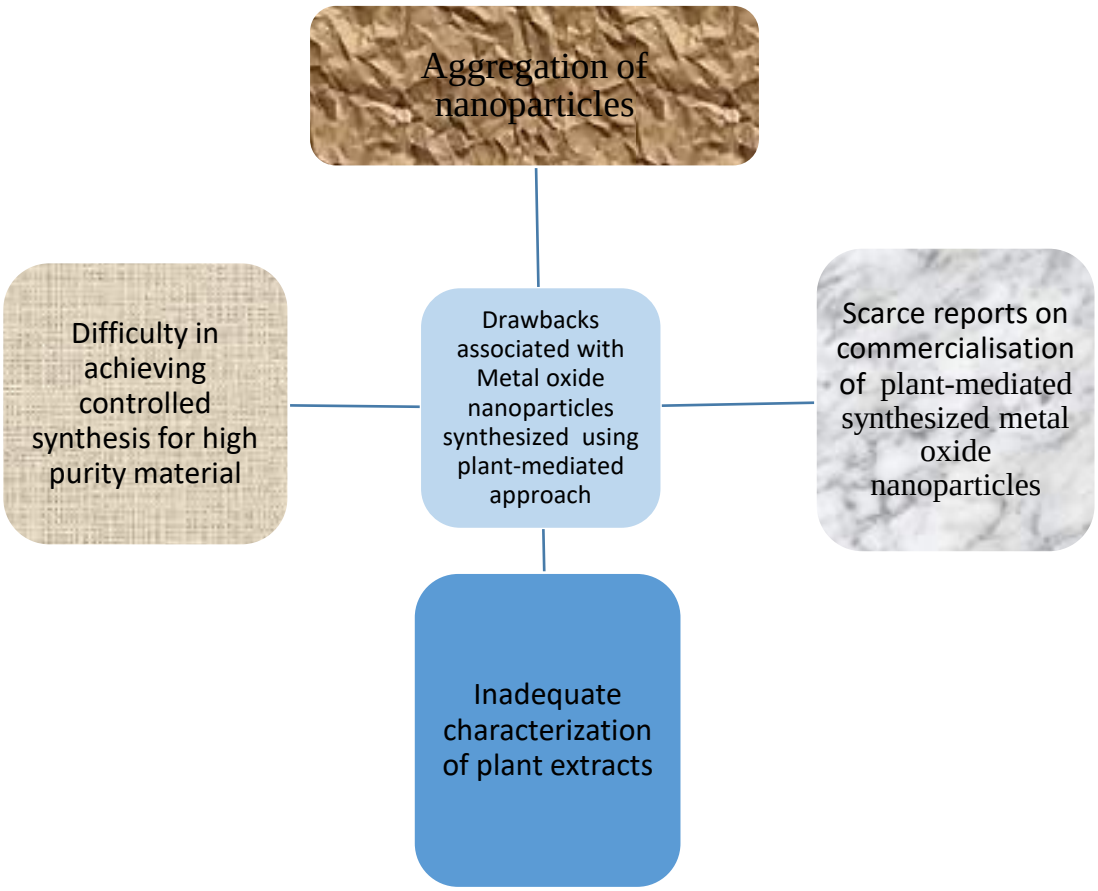

Figure 8. Challenges associated with Metal oxide nanoparticles synthesized using plant-mediated approach

Conclusion

The use of extracts of plants for synthesis of transition metal oxide nanoparticles is simple, inexpensive, environmental friendly and easy to adopt for industrial scale production. Conditions such as pH, reaction time, reaction temperature, extract-metal precursor volume ratio, concentration of metal precursor and calcination temperature have a tremendous influence on the properties of the synthesized metal oxide nanoparticles. Metal oxide nanoparticles synthesized via this approach have been employed for various applications including drug delivery, antioxidant, antibacterial, electrochemical applications, photocatalysis, sensors, immobilization of enzyme, adsorption of dyes and heavy metals from aqueous systems. Reduction potential differs from one plant to another. However, the use of plant extracts for synthesis of metal oxide nanoparticles is not devoid of shortcomings such as aggregation of nanoparticles and difficulty in achieving controlled synthesis so as to obtain high purity nanoparticles that are devoid of structural defects. Improving on these shortcomings would be an extraordinary breakthrough in this area. Transition metal oxide nanoparticles synthesized using plant extracts are crystalline in most cases and even agglomerated forms of metal oxide nanoparticles synthesized using extracts of plants are efficient for some applications. Compositing affects the shape and efficiency of metal oxide nanoparticles. Deductions from comparison of some reports suggest that application of these nanoparticles depend on parameters such as crystal structure, crystalline size and morphology since metal oxide nanoparticles reported to be efficient for specific application share similar attributes.

REFERENCES

Abomuti, M. A., Danish, E. Y., Firoz, A., Hasan, N., Malik, A. M. (2021). Green Synthesis of Zinc Oxide Nanoparticles Using Salvia officinalis Leaf Extract and Their Photocatalytic and Antifungal Activities. *Biology*, 10, 1075. https://doi.org/10.3390/biology10111075.

Ahmad, W., Bhatt, S. C., Verma, M., Kumar, V. and Kim, H. (2022). A review on current trends in the green synthesis of nickel oxide nanoparticles, characterizations, and their applications. *Environmental Nanotechnology, Monitoring & Management*, 18, 100674. https://doi.org/10.1016/j.emmm.2022.100674.

Akhir, R. M., Norashikin, M. H. Mahat, M. M., Bonnia, N. N. (2019). Biosynthesis of zinc oxide nanoparticles for corrosion protection application. *International Journal of Engineering & Technology* 7(4.14): 488-492. DOI: https://doi.org/10.14419/ijet.v7i4.14.27775.

Akhtar, N., Khan, S., Rehman, S. U., Rehman Z. U., Mashwani, Z. R., Rha, E. S. and Jamil, M. (2021). Zinc Oxide nanoparticles enhance the tolerance and remediation potential of Bacillus spp. against heavy metal stress. *Adsorption Science & Technology*, 177452. https://doi.org/10.1155/2021/177452

Alamdari, S., Ghamsari, S. M., Lee, C., Han, W., Park, H.H., Tafreshi, M.J., Afarideh, H., Ara, M.H.M. (2020). Preparation and characterization of zinc oxide nanoparticles using leaf extract of Sambucus ebulus. *Appl. Sci.* 10 3620. https://doi.org/10.3390/app10103620.

Altikatoglu, M., Attar, A., Erci, F., Cristache, C. M., Isildak, I., (2017). Green synthesis of copper oxide nanoparticles using ocimum basilicum extract and their antibacterial activity, *Fresenius Environmental Bulletin*, 26(12): 7832-7837.

Amin, F., Fozia, Khattak, B., Alotaibi, A., Qasim, M., Ahmad, I., Ullah, R., Bourhia, M., Gul, A., Zahoor, S. and Ahmad R. (2021). Green Synthesis of Copper Oxide Nanoparticles Using Aerva javanica Leaf Extract and Their Characterization and Investigation of invitro Antimicrobial Potential and Cytotoxic Activities. *Evidence-based complementary and alternative medicine*, 5589703. https://doi.org/10.1155/2021/5589703

Andualem, W. W., Sabir, F. K., Mohammed, E. T., Hadgu, H. B., Bedasa, A. G., (2020). Synthesis of copper oxide nanoparticles using plant leaf extract of catha edulis and its antibacterial activity. *Journal of Nanotechnology*, 2932434. https://doi.org/10.1155/2020/2932434

Aslam, R., Mobin, M., Shoeb, M., Aslam J. (2022). Novel ZrO2-glycine nanocomposite as eco-friendly high temperature corrosion inhibitor for mild steel in hydrochloric acid solution. *Scientific Reports,* 12:9274. https://doi.org/10.1038/s41598-022-13359-y.

Aziz, R. A., Bronny, B. G., (2019). Zinc oxide nanoparticle synthesis with banana peel extract from jackfruit banana: effects of temperature. *International journal for technological research in engineering*, 26-30. www.ijtre.com.

Aziz, W. J., Abid, M. A., Kadhim, D. A., Mejbe, M. K., (2020). Synthesis of iron oxide (β-Fe_2O_3) nanoparticles from Iraqi grapes extract and its biomedical application. *Materials Science and Engineering IOP Conf. Series* 881. doi:10.1088/1757-899X/881/1/012099.

Baig, N., Kammakakam, I., Falath, W. (2022). Nanomaterials: a review of synthesis methods, properties, recent progress, and challenges. *Mater. Adv.*, 2, 1821–1871. DOI: 10.1039/d0ma00807a

Barzinjy, A. A., Azeez, H. H., (2020). Green synthesis and characterization of zinc oxide nanoparticles using Eucalyptus globulus Labill. leaf extract and zinc nitrate hexahydrate salt. *Springer nature journal*, 2:991. https://doi.org/10.1007/s42452-020-2813-1.

Bashir, M., Riaz, S., Naseem, S., (2013). Effect of pH on ferromagnetic iron oxide nanoparticles, *International Conference on Solid State Physics (ICSSP'13)*. doi:10.1016/j.matpr.2015.11.106.

Basri, H. H., Talib, R. A., Sukor, R., Othman, S. H., Ariffin, H., (2020). Effect of Synthesis Temperature on the Size of ZnO Nanoparticles Derived from Pineapple Peel Extract and Antibacterial Activity of ZnO–Starch Nanocomposite Films. *Nanomaterials*, 10. doi:10.3390/nano10061061.

Begum, S. N., Esakkiraja, A., Asan, S. M., Muthumari, M., Raj, G. V., (2019). Green Synthesis of Copper Oxide Nanoparticles Using Catharanthus Roseus Leaf Extract and Their Antibacterial Activity. *International Journal of Scientific Research in Multidisciplinary Studies*, 5(8): 21-27. Available online at: www.isroset.org.

Bepari, R.A., Bharali P., Das, B. K., (2014). Controlled synthesis of a- and c-Fe2O3 nanoparticles via thermolysis of PVA gels and studies on a-Fe2O3 catalyzed styrene epoxidation. *Journal of Saudi Chemical Society*, 21: 170-178. http://dx.doi.org/10.1016/j.jscs.2013.12.010.

Buarki, F., AbuHassan, H., Hannan, F. A. and Henari, F. Z. (2022). Green Synthesis of Iron Oxide Nanoparticles Using Hibiscus rosa sinensis Flowers and Their Antibacterial Activity. *Journal of Nanotechnology*, 5474645. https://doi.org/10.1155/2022/5474645

Chung, M., Rahuman, A., Marimuthu, S., Kirthi, A.K., Anbarasan, P., Rajakumar, P. G. (2017). Green synthesis of copper nanoparticles using Eclipta prostrata leaves extract and their antioxidant and cytotoxic activities. *Exp. Ther Med*, 14: 18–24. https://doi.org/10.3892/etm.2017.4466.

Datta, A., Patra, C., H. Bharadwaj, S. Kaur, N. Dimri, R. Khajuria, (2017). Green Synthesis of Zinc Oxide Nanoparticles Using Parthenium hysterophorus Leaf Extract and Evaluation of their Antibacterial Properties. *J. Biotechnol. Biomater*, 7: 3–7. https://doi.org/10.4172/2155-952x.1000271.

Demissie, M. G., Sabir, F. K., Edossa G. D., Gonfa B. A., (2020). Synthesis of Zinc Oxide Nanoparticles Using Leaf Extract of Lippia adoensis (Koseret) and Evaluation of Its Antibacterial Activity. *Journal of Chemistry*, 7459042. https://doi.org/10.1155/2020/7459042.

Devatha, C. P., Thalla, A. K., Katte, S. Y. (2016). Green synthesis of iron nanoparticles using different leaf extracts for treatment of domestic waste water, Journal of Cleaner Production. *Journal of Cleaner Production*. doi:10.1016/j.jclepro.2016.09.019.

Devi, K. S., Singh, A. R., Velmurugan, D., Devi, D., Lourembam, D. S., Singh, N. R., (2021). Green Synthesis of Copper Oxide Nanoparticles Using Coix lacryma jobi Leaves Extract and Screening of its Potential Anticancer Activities. *Journal of pharmaceutical research international*, 33: 128-139. DOI: 10.9734/JPRI/2021/v33i52A33566.

Dobrucka, R., Długaszewska, J. (2016). Biosynthesis and antibacterial activity of ZnO nanoparticles using Trifolium pratense flower extract. *Saudi J. Biol. Sci.*, 23, 517–523. https://doi.org/10.1016/j.sjbs.2015.05.016.

Drummer, S., Madzimbamuto, T., and Chowdhury M., (2021). Green Synthesis of Transition Metals Nanoparticle and their Oxides: A Review. *Materials (Basel)*, 14(11): 2700. doi:10.3390/ma14112700.

Elumalai, K., Velmurugan, S., Ravi, S., Kathiravan, V., Ashokkumar, S. (2015). Facile, ecofriendly and template free photosynthesis of cauliflower like ZnO nanoparticles using leaf extract of Tamarindus indica (L.) and its biological evolution of antibacterial and antifungal activities. *Spectrochim. Acta - Part A Mol. Biomol. Spectrosc*, 136:

1052–1057. https://doi.org/10.1016/j.saa.2014.09.129.

Fagier, M. A., (2021). Plant-Mediated Biosynthesis and Photocatalysis Activities of Zinc Oxide Nanoparticles: A Prospect towards Dyes Mineralization. *Journal of Nanotechnology*, 6629180. https://doi.org/10.1155/2021/6629180

Faisal, S., Jan, H., Shah, A. S., Shah S., Khan, A., Akbar, T. M., Rizwan, M., Jan, F., Wajidullah, Akhtar, N., Khattak, A., Syed S., (2021). Green synthesis of zinc oxide (ZnO) nanoparticles using aqueous fruit extracts of myristica fragrans: their haracterizations and biological and environmental applications. *ACS Omega*, 6: 9709−9722. https://doi.org/10.1021/acsomega.1c00310.

Fakhari, S., Jamzad M., Fard, K. H., (2019). Green synthesis of zinc oxide nanoparticles: a comparison, *Green Chemistry Letters and Reviews*, 12(1): 19-24. DOI:10.1080/17518253.2018.1547925.

Fardood, S.T., Ramazani, A., Moradi, S., Asiabi, P.A. (2017). Green synthesis of zinc oxide nanoparticles using Arabic gum and photocatalytic degradation of direct blue 129 dye under visible light, *J. Mater. Sci. Mater. Electron*. 28, 13596–13601. https://doi.org/10.1007/s10854-017-7199-5.

Gurgur, E., Oluyamo, S. S., Adetuyi, A. O., Omotunde, O. I., Okoronkwo, A. E., (2020). Green synthesis of zinc oxide nanoparticles and zinc oxide–silver, zinc oxide–copper nanocomposites using *Bridelia ferruginea* as biotemplaten. *SN Applied Sciences* 2:911. https://doi.org/10.1007/s42452-020-2269-3.

Guzman, M., Arcos, M., Dille, J., Rousse, C., Godet, S., Malet, L. (2021). Effect of the Concentration and the Type of Dispersant on the Synthesis of Copper Oxide Nanoparticles and Their Potential Antimicrobial Applications. *ACS Omega*, 6: 18576−18590. https://doi.org/10.1021/acsomega.1c00818

Habtemariam, A. B., Oumer, M. (2020). Plant Extract Mediated Synthesis Of Nickel Oxide Nanoparticles. *Materials international*, 2(2): 0205-0209.

Hafeez, M., Shaheen, R., Akram, B., Zain-ul-Abdin, Haq, S., Mahsud, S., Ali, S., Khan, R. T. (2020). Green synthesis of cobalt oxide nanoparticles for potential biological applications. *Mater. Res. Express*, 7: 1-8. https://doi.org/10.1088/2053-1591/ab70dd.

Haider, A., Ijaz, M., Ali, S., Haider, J., Imran, M., Majeed, H., Shahzadi, I., Ali, M. M., Khan, J. A., Ikram M. (2020). Green Synthesized Phytochemically (Zingiber officinale and Allium sativum) Reduced Nickel Oxide Nanoparticles Confirmed Bactericidal and Catalytic Potential. *Nanoscale Research*, 15(50): 1-11. https://doi.org/10.1186/s11671-020-3283-5.

Ijaz, F., Shahid, S., Khan, S. A., Ahmad W., Zaman, S., (2017). Green synthesis of copper oxide nanoparticles using Abutilon indicum leaf extract: Antimicrobial, antioxidant and photocatalytic dye degradation activities. *Tropical journal of pharmaceutical research*, 4: 743-75. http://dx.doi.org/10.4314/tjpr.v16i4.2.

Jayachandran, A., Aswathy T.R., and Achuthsankar, S. N., (2021). Green synthesis and characterization of zinc oxide nanoparticles using Cayratia pedata leaf extract. *Biochemistry and Biophysics Reports* 26, 1-8. https://doi.org/10.1016/j.bbrep.2021.100995.

Karnan, T., Selvakumar, S.A.S. (2016). Biosynthesis of ZnO nanoparticles using rambutan (Nephelium lappaceum L.) peel extract and their photocatalytic activity on methyl orange dye. *Journal of molecular structure*, 1125, 358-365. https://doi.org/10.1016/j.molstruc.2016.07.029.

Kiwumulo, H. F., Muwonge, H., Ibingira, C., Lubwama, M., Kirabira, J. B., Ssekitoleko R. T., (2022). Green synthesis and characterization of iron-oxide nanoparticles using

Moringa oleifera: a potential protocol for use in low and middle income countries. *BMC Research Notes*, 15, 149. https://doi.org/10.1186/s13104-022-06039-7

Lakshminarayanan, S., Shereen, M. F., Niraimathi, K. L., Brindha, P., Arumugam, A., (2021). One-pot green synthesis of iron oxide nanoparticles from Bauhinia tomentosa: Characterization and application towards synthesis of 1, 3 diolein. *Scientific Reports*, 11: 8643. https://doi.org/10.1038/s41598-021-87960-y.

Lefojane, R., Direko, P., Mfengwana, P., Mashele, S., Matinise, N., Maaza, M., Sekhoacha, M. (2020). Green Synthesis of Nickel Oxide (NiO) Nanoparticles Using Spirostachys africana Bark Extract. *Asian Journal of Scientific Research*, 13: XX-XX. DOI: 10.3923/ajsr.2020.XX.XX.

Lu, J., Batjikh, I., Hurh, J., Han, Y., Ali, H., Mathiyalagan, R., Yang, D.C. (2019). Photocatalytic degradation of methylene blue using biosynthesized zinc oxide nanoparticles from bark extract of Kalopanax septemlobus. *Optik* 182: 980–985. https://doi. org/10.1016/j.ijleo.2018.12.016.

Maham, M., Sajadi, S.M., Kharimkhani, M.M. Nasrollahzadeh, M. (2017). Biosynthesis of the CuO nanoparticles using Euphorbia Chamaesyce leaf extract and investigation of their catalytic activity for the reduction of 4-nitrophenol. *IET Nanobiotechnology*, 11: 766–772. https://doi.org/10.1049/iet-nbt.2016.0254.

Naseer, M., Aslam, U., Khalid, B., Chen B., (2020). Green route to synthesize Zinc oxide nanoparticles using leaf extracts of Cassia fistula and Melia azadarach and their antibacterial potential. *Scientific reports*, 10:9055. https://doi.org/10.1038/s41598-020-65949-3

Nguyen, N. T., Nguyen, V. A. (2020). Synthesis, Characterization, and Photocatalytic Activity of ZnO Nanomaterials Prepared by a Green, Nonchemical Route. *Journal of Nanomaterials*, 1768371. https://doi.org/10.1155/2020/1768371

Nhu, V. T., Dat, N. D., Tam, L., Phuong, N. H., (2022). Green synthesis of zinc oxide nanoparticles toward highly efficient photocatalysis and antibacterial application. *Beilstein J. Nanotechnol*, 13: 1108–1119. https://doi.org/10.3762/bjnano.13.94

Niraimathee, V.A., Subha, V., Ravindran R.S., Renganathan S. (2016). Green synthesis of iron oxide nanoparticles from Mimosa pudica root extract. *Int. J. Environment and Sustainable Development*, 15(3): 227-240. https://doi.org/10.1504/IJESD.2016.077370.

Nwanya, A. C., Botha, S., Ezema, F. I., Maaza M., (2021). Functional metal oxides synthesized using natural extracts from waste maize materials. *Current-research-in-green-and-sustainable-chemistry* 4, 1-18. https://doi.org/10.1016/j.crgsc.2021.100054.

Osuntokun, J., Onwudiwe, D.C., Ebenso, E.E. (2019). Green synthesis of ZnO nanoparticles using aqueous Brassica oleracea L. var. italica and the photocatalytic activity. *Green Chem. Lett. Rev.*, 12: 444–457. https://doi.org/10.1080/ 17518253.2019.1687761.

Pradhan, S., Shrestha, R., Bhandari, K., (2020) Effect of various parameters on bio-synthesis of copper nanoparticles using citrus medica linn (lemon) extract and its antibacterial activity. *Amrit Resarch Journal*, 1(1): 51-58.

Prasad, K.S., Patra, A., Shruthi, G. Chandan, S. (2017). Aqueous extract of *saraca indica* leaves in the synthesis of copper oxide nanoparticles: Finding a way towards going green. J. Nanotechnol. 2017 https://doi.org/10.1155/2017/7502610.

Primo, J.d., Bittencourt, C., Acosta, S., Sierra-Castillo, A., Colomer, J. F., Jaerger, S., Teixeira, V. C., and Anaissi, F. J. (2020). Synthesis of zinc oxide nanoparticles by ecofriendly routes: adsorbent for copper removal from wastewater. *Front. Chem.*, 8.571790. doi: 10.3389/fchem.2020.571790.

Qu, J., Yuan, X., Wang, X., Shao, P. (2011). Zinc accumulation and synthesis of ZnO nanoparticles using Physalis alkekengi L. *Environ. Pollut*. 159, 1783–1788.

https://doi.org/10.1016/j.envpol.2011.04.016.

Raj, A., Lawerence R., (2018). Green synthesis and characterization of ZnO nanoparticles from leafs extracts of rosa indica and its antibacterial activity. *Asayan J. Chem*, 11(3): 1339-1348. http://dx.doi.org/10.31788/RJC.2018.1132009.

Ramesh, M., Anbuvannan, M., Viruthagiri, G. (2015). Green synthesis of ZnO nanoparticles using Solanum nigrum leaf extract and their antibacterial activity. *Spectrochim. Acta A Mol. Biomol. Spectrosc.* 136, 864–870.https://doi.org/10.1016/J.SAA.2014.09.105.

Razack, S. A., Suresh, A., Sriram, S., Ramakrishnan, G., Sadanandham, S., Veerasamy, M., Nagalamadaka, R. B., Sahadevan, R., (2020). Green synthesis of iron oxide nanoparticles using Hibiscus rosa-sinensis for fortifying wheat biscuits. *SN Applied Sciences* 2, 898, https://doi.org/10.1007/s42452-020-2477-x.

Rose, A. A., Sheeja, K. R., (2021). Green synthesis, characterization and photocatalytic activity of cobalt and zinc oxide nanoparticles functionalised starch nanocomposite. *European journal of molecular & clinical medicine*, 8(2): 1606-1617.

Sahoo, S.K., Agarwa, K., Singh, A.K., Polke, B.G., Raha, K.C., (2010). Characterization of γ- and α-Fe_2O_3 nano powders synthesized by emulsion precipitation-calcination route and rheological behaviour of α-Fe_2O_3. *International Journal of Engineering, Science and Technology*, 2, 118-126. www.ijest-ng.com.

Saranya, S., Vijayarani K., Pavithra, S., (2017). Green synthesis of iron nanoparticles using aqueous extract of Musa Ornata Flower Sheath against Pathogenic Bacteria. *Indian journal of pharmaceutical sciences* 9(5): 688-694.

Sardjono, S. A., Puspitasari, P., (2020). Synthesis and Characterization of Cobalt Oxide Nanoparticles Using Sol-Gel Method. *AIP Conference Proceedings*, 2231, 1-4. https://doi.org/10.1063/5.0002419.

Sharmila, G., Pradeep, R. S., Sandiya, K., Santhiya, S., Muthukumaran, C., Jeyanthi, J., Kumar, N. M., Thirumarimurugan, M. (2018). Biogenic synthesis of CuO nanoparticles using Bauhinia tomentosa leaves extract: Characterization and its antibacterial application. *J. Mol. Struct.*, 1165, 288–292. https://doi.org/10.1016/j.molstruc.2018.04.011.

Shreema, K., Mathammal, R., Kalaiselvi, V., Vijayakumar, S., Selvakumar, K., Senthi, K., (2021) Green synthesis of silver doped zinc oxide nanoparticles using fresh leaf extract Morinda citrifoliaand its antioxidant potential. *Materials Today*: Proceedings 47(9): 2126-2131. https://doi.org/10.1016/j.matpr.2021.04.627.

Sukumar, S., Rudrasenan, A., Nambiar, D. P., (2020). Green-Synthesized Rice-Shaped Copper Oxide Nanoparticles Using Caesalpinia bonducella Seed Extract and Their Applications. *ACS Omega*, 5, 1040−1051. DOI: 10.1021/acsomega.9b02857.

Sulaiman, G., Tawfeeq, A., Jaaffer, M. (2017) Biogenic synthesis of copper oxide nanoparticles using Olea europaea leaf extract and evaluation of their toxicity activities: An in vivo and in vitro study. *Biotechnol. Prog.*, 34(1), 218-230. https://doi.org/10.1002/btpr.2568

Sangeetha, G., Rajeshwari, S., Venckatesh, R. (2011) Green synthesis of zinc oxide nanoparticles by aloe barbadensis miller leaf extract: Structure and optical properties. *Mater. Res. Bull.*, 46: 2560–2566. https://doi.org/10.1016/j.materresbull.2011.07.046.

Surendhiran, S., Gowthambabu, V., Balamurugan, A., Sudha, M. Kumar, V.B., Suresh, K.C. (2021). Rapid green synthesis of CuO nanoparticles and evaluation of its photocatalytic and electrochemical corrosion inhibition performance. *Materials today: Proceedings*, 47(4): 1011-1016. https://doi.org/10.1016/j.matpr.2021.05.515.

Tas, R., Koroglu, E., Celebioglu, H. U., (2021) Green synthesis of nickel nanoparticles using peumus boldus koch. extract and antibacterial activity. *International Journal of*

Innovative Engineering Applications 5(2), 152-155. Doi:https://doi.org/10.46460/ijiea.929625.

Tuček, J., Machala, L., Ono S., Namai, A., Yoshikiyo, M., Imoto, K., Tokoro, H., Ohkoshi, S., Zbořil, R., (2015). Zeta-Fe_2O_3 – A new stable polymorph in iron(III) oxide family. *Scientific reports*, 5, 15091. DOi: 10.1038/srep15091.

Umar, H., Kavaz, D., Rizane, N., (2019). Biosynthesis of zinc oxide nanoparticles using Albizia lebbeck stem bark, and evaluation of its antimicrobial, antioxidant, and cytotoxic activities on human breast cancer cell lines. *International Journal of Nanomedicine*, 14: 87–100. http://dx.doi.org/10.2147/IJN.S186888.

Üstün, E., Önbaş, S. C., Celik, S. K., Ayvaz, M. C., Sahin, N., (2022). Green Synthesis of Iron Oxide Nanoparticles by Using Ficus Carica Leaf Extract and Its Antioxidant Activity. *Biointerface research in applied chemistry*, 12(2): 2108 – 2116. https://doi.org/10.33263/BRIAC122.21082116.

Wardani, M., Yulizar, Y., Abdullah, I., Apriandanu, D. O., (2019). Synthesis of NiO nanoparticles via green route using Ageratum conyzoides L. leaf extract and their catalytic activity. *IOP Conf. Ser.: Mater. Sci. Eng*., 509, 012077. doi:10.1088/1757-899X/509/1/012077.

Waris, A., Din, M., Ali, A., Afridi, S., Baset, A., Khan, A. U., Ali, M., (2021). Green fabrication of Co and Co_3O_4 nanoparticles and their biomedical applications: A review. *Open life sciences*, *16*(1), 14–30. https://doi.org/10.1515/biol-2021-0003.

Xu, J., Huang, Y., Zhu, S., Abbes, N., Jing, X., and Zhang, L. (2021). A review of the green synthesis of ZnO nanoparticles using plant extracts and their prospects for application in antibacterial textiles. *Journal of Engineered Fibers and Fabrics*, 16, 1–14. DOI:10.1177/15589250211046242.

Yedurkar, S., Maurya, C., Mahanwar P., (2016). Biosynthesis of Zinc Oxide Nanoparticles Using Ixora Coccinea Leaf Extract—A Green Approach. *Open Journal of Synthesis Theory and Applications*, 5: 1-14. http://dx.doi.org/10.4236/ojsta.2016.51001.

Yonti, C., Kenfack Tsobnang, P., Lontio Fomekong, R., Devred, F., Mignolet, E., Larondelle, Y., Hermans, S., Delcorte, A., Lambi Ngolui, J., (2021). Green Synthesis of Iron-Doped Cobalt Oxide Nanoparticles from Palm Kernel Oil via Co-Precipitation and Structural Characterization. *Nanomaterials*, 11, 2833, 1-20. https://doi.org/10.3390/nano11112833.

Yusoff, A. H., Salimi, M. N., Jamlos, M. F., (2017). Synthesis and Characterization of Biocompatible Fe_3O_4 Nanoparticles at Different pH. *Advanced Materials Engineering and Technology AIP Conference Proceedings*, 1835, https://doi.org/10.1063/1.4981832.

Zayyoun, N., Bahmad, L., Laaˆnab, L. and Jaber, B. (2016). The effect of pH on the synthesis of stable Cu_2O/CuO nanoparticles by sol–gel method in a glycolic medium. *Appl. Phys. A*, 122(488) 1-6. DOI 10.1007/s00339-016-0024-9.